Fall 12-18-2019

The Scaffolds to Guide Fast Angiogenesis

Tianhong Zhou
Washington University in St. Louis

WASHINGTON UNIVERSITY IN ST. LOUIS

Division of Material Science and Engineering

Dissertation Examination Committee:
Jianjun Guan
Spencer Lake
Jie Shen

The Scaffolds to Guide Fast Angiogenesis

by
Tianhong Zhou

A dissertation presented to
McKelvey School of Engineering
of Washington University in
partial fulfillment of the
requirements for the degree
of Master of Material Science and Engineering

December 2019
St. Louis, Missouri

Table of Contents

List of Figures

List of Tables

Acknowledgments

Thanks to the cooperation from Professor Shen's lab in School of Medicine School at Washington University in Saint Louis did the vivo experiments and Professor Lake's lab in MEMS at Washington University for tensile test machine.

I would like to express my special thanks of gratitude to my PI Doctor Guan as well as lab members who gave me the golden opportunity to do this wonderful project on the biomaterial, which also helped me in doing a lot of Research I am really thankful to them. Secondly, I would also like to thank my parents and friends who helped me a lot in finalizing this project within the limited time frame.

Tianhong Zhou

Washington University in St. Louis

December 2019

Dedicated to my parents.

The Scaffolds to Guide Fast Angiogenesis

by

Tianhong Zhou

Master of Material Science and Engineering

Washington University in St. Louis, 2019

Professor Jianjun Guan,

Angiogenesis is one of the most challenging problems in bone structure repair. The different types of 3D fibrous morphology structure of the extracellular matrix for fasting angiogenesis have been studied. Due to the densely packed constructs and limited porosity of scaffold, the challenge still remains for scaffold fabrication. In this study, we fabricated PCL scaffold with growth factors and cells to guide fast angiogenesis by electro-spinning and electro-spray simultaneously. We developed a technique that electro-spinning encapsulates growth factors OPN(Recombinant Human Osteopontin) and SDF-1α(CXCL12) in poly(lactide-co-glycolide) (PLGA) microspheres into PCL 3D structures scaffold fibers. We also developed a new technique to fabricated cells into PCL scaffold coating with gelatin A. And tested release amount of growth factors in scaffold over 28 days and loading efficiency. We can prove that microsphere released growth factors successfully into release medium in vitro. The Young's module and elongation rate been tested by the single axis tensile test. The migration in collagen gel and in fibers were tested and quantified by confocal fluorescence microscopy. In vitro cell migration study demonstrated that OPN and SDF-1 significantly increased the depth of cell migration. In vivo, the scaffold with growth factors improve the repair of bone fracture in RA mice. Based on the results, these 3D scaffold may have potential to engineer tissues for various applications.

Chapter 1: Introduction

For now, healing of bone fractures and reconstruction of bone defects represent a significant challenge. The goal of tissue engineering is to bring together cells, tissue scaffolds, and a combination of electrical, mechanical, or chemical cues to stimulate the repair or regeneration of tissue. Guided tissue regeneration technologies are a frequently used standard procedure for bone regeneration therapy in the animal. For tissues implanting into human, due to the lack of nutrients and supply of cells in the scaffold, cell implanting tissues are always facing problems about poor locations or wrong volume issues.[1,2] Bone fracture repair occurs through a complex serious of events that lead to regeneration of bone with mechanical strength and tissue morphometry. During endochondral healing, the mesenchymal cells, upon receiving differentiation cues, undergo chondrogenesis to form a cartilaginous soft callus primarily in the more hypoxic environment lacking blood vessels. So blood vessel formation is important for fracture repair. In some cases, although the natural formation of angiogenesis caused by the body's inflammatory response can make angiogenesis supply nutrients to the cells, this process is usually too slow, or the density of the blood vessels generated is too low to provide enough nutrition.[3] In addition, the regenerative blood vessels generated in the process of natural angiogenesis are limited to the regeneration of peripheral blood vessels and cannot be evenly distributed inside the tissue to achieve the purpose of nutrition transportation. Therefore, rapid angiogenesis in guiding structures during tissue regeneration is critical. Angiogenesis growth factors are proved to be stimulated for vessel formation. [3]

1.1 Introduction

Various studies have demonstrated that delivering angiogenic growth factors could accelerate angiogenesis. [4,5] One of the most efficient ways of stimulating angiogenesis is delivering angiogenic growth factors into the animal directly.

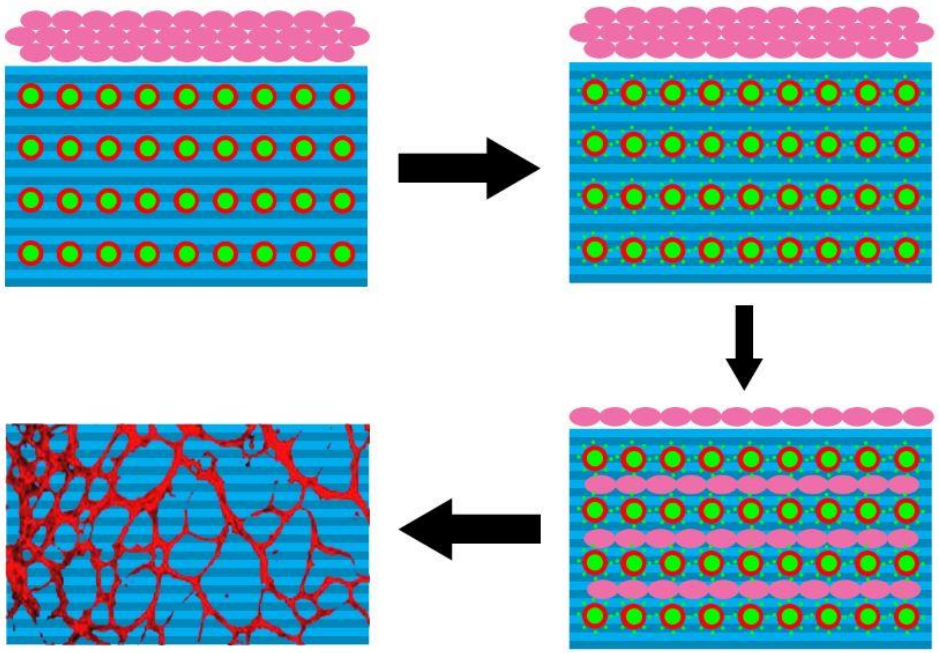

figure 1.1a: Scaffold with microspheres release model in vivo

Figure 1.1a is the model of the scaffold fabricated for releasing growth factors and improving the formation of blood vessels in vivo experiments. The background represents the scaffold which is oriental PCL polymer fibers in this case. The red-green microspheres represent polymer encapsulated growth factors, which are the key factors for releasing growth factors and improving blood vessel regeneration. As figure 1.1 shown above, the growth factors in the tissue regeneration scaffold released in vivo. Cells outside the scaffold migrate into the scaffold with the stimulation of growth factors. Eventually, the blood vessel formation in the biodegradable scaffold and new tissue regenerated. [6]

For tissue regeneration, there are several methods to deliver growth factors into human directly. Such as hydrogel porous scaffold, which could solve the problem of the short half-life of growth factors in vivo situation. But it still cannot solve the challenge of establishing vessel in short time and cannot offer structure support for new formed tissues. [7] So, creating controllable growth factors release system could be vital for tissue regeneration. That is the reason we introduced the 3D porous scaffolds for loading growth factors and cells, which could create well-defined density of ingredients continually. [8,9,10,11] Also, the formation of blood vessel in regenerated tissues will indirectly affect the cells' migration process, which will be discussed in detail in next part. But there is some feedback for growth factors delivering process. In this project, we employed electro-spinning and electro-spray method to improve the effective and try to control growth factors release rate.

1.2 Core-Shell Microsphere Structure for Drug Delivery

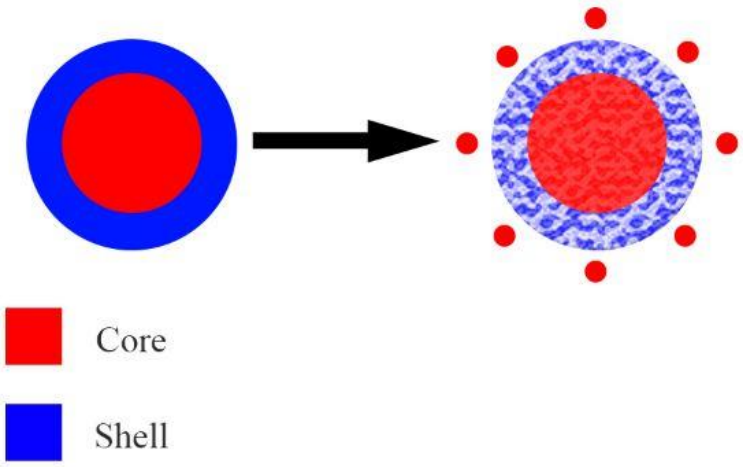

Figure 1.2 Encapsulated microsphere degradation process

A major problem preventing the progression of protein-based drugs microparticle delivery is the issue of their stability and release rate during microencapsulation in vivo. [6] As the figure 1.2 shown, the red part represent drug encapsulated in polymer shell. After degrading of polymer in animal body or solution environment, the drug release from inside in controllable rate. As a result, solid degradable microsphere considered to be one of the most effectiveness therapeutic method to be loading drug into animals' body for several advantages. Firstly, because of the small size, they can dissolve in loading materials and improving drug stability and extent drug bioactivity. Secondly, with the coating of polymer shell, drug in core could avoid adverse effects and unwanted degradation in advanced. Thirdly, microsphere could load various drugs such as growth factors, anti-body and other proteins. According to recent research, variety of polymers could be employed to make shell structure for loading drug such as PGA and PLGA and PCL. [12]

Not only the polymer material of shell could affect the drug loading property of microsphere, the morphology of polymer covering the drug inside. According to recent studies, morphology of microsphere influences the mechanism of drug delivery in many methods. [13] Firstly, polymer matrix affects the kinetic of microsphere shell degradation because of the different surface reactivity of polymer. Also, polymer particles could influence the circulation of drug release inside the polymer due to the chemical property. Finally, the local shape of microsphere could influence the binding in vivo cause the binding site of macrophage internalization. Different morphology of microspheres will lead to different surface affinities anchored on the target cells, spherical particles and disc-shaped particles are taken as an example. According to research, the disc-shaped particles have a larger surface area compare to spherical sphere. Particles with large surface-to-volume ratios are preferred for targeting because large surfaces allow conjugation of many ligands., which explains why the adsorption efficiency of discoid particles is much higher than that of spherical particles.

CXCL12(Stromal cell-derived factor 1) also known as C-X-C motif chemokine 12 (CXCL12), is a chemokine protein that expressed in humans by the CXCL12 gene on chromosome 10th. The function of CXCL12 is that it could directs the migration of hematopoietic cells during the embryogenesis from the liver to the bone marrow and the formation of blood vessels. Osteopontin (OPN), also known as bone sialoprotein I (BSP-1), is a highly negatively charged protein. OPN is a phosphorylated glycoprotein that binds integrins and functions as a mediator of cell adhesion, migration, immune responses, and tissue repair. In the process of angiogenesis, the lack of OPN and CXCL12 is the mainly reason of lack of blood vessel formation. [14] Previously research proved that the recombinant mouse CXCL12/SDF-1a and recombinant mouse osteopontin/OPN, which were used at the final concentration of 100 ng/mL and 500 ng/mL could

improve the HUVEC tube formation and cell migration assays in vivo experiment. [15] Importantly, with the combination of protein provide better improvement for blood vessel formation. In this project, we followed the proportion of two growth factors in the previous study. Recent study proved that Dnmt3b deficiency in chondrocytes results in hypertrophic maturation delay and thus leads to vasculogenic response delay to injury likely via downregulation of certain key angiogenic factors, primarily CXCL12 and OPN. So the defects in tube formation and cell migration could be rescued by administration of CXCL12 and OPN. The proportion kept in 1:5 for SDF-1 and OPN in electro-spray process.

Adipose Tissue-derived Stem Cell (ADSC) are human adult stem cells isolated from fat tissues during procedures such as liposuction, abdominoplasty, or breast reduction and can be used to promote skin and hair growth. ADSCs have been proved that could isolated to blood vessel in vivo and in vitro. [16] In this project, we fabricated ADSCs in PCL scaffold by electro-spinning and try the best to keep bioactivity under high voltage during electro-spinning process in chapter 3.

1.3 Electro-spray Method

Electrostatic spray, also known as Electrohydrodynamic liquid atomization (EHDA), is a method of dispersing molten liquid or liquid solution into small pieces using electrostatic field force. [17] Generally, higher voltages are applied to the liquid in the tube through a thinner glass or metal tube. Under appropriate conditions, the liquid will be inserted into the end of the tube and form a Taylor vertebra. The tail end will form a jet-like thin line and atomize, and the tail end of the thin line will be quickly released drop by drop. [18] Electrostatic spray is based on the basic principle of the existence of thousands of digits of primary surface energy, which breaks into small

protrusions under the action of Coulomb's substitution force. In 1882, Lord Rayleigh theoretically estimated the maximum amount of charge that a droplet can carry. This amount is called the "Rayleigh limit". If the surface charge of a droplet exceeds this limit, the droplet will be broken into smaller particles. And found that almost all fluids can successfully achieve electrostatic spraying under high voltage. [19]

In electro-spray, if a certain particles or polymer is dissolved in solution in advance to make a precursor solution, the precursor solution is pushed out of a charged needle by gravity or other force. Under the proper electric field conditions, the trailing end forms a thin jet-like line, the liquid filament will be broken into very fine droplets. And as the solvent in the droplets evaporates, the droplets gradually become micro- or nano-scale solid particles, and finally deposit on the substrate collectors. [20] In addition, once the type and physical and chemical properties of the solution are determined and the conditions of the electro-spray are determined, the morphology and size of each solid particle should theoretically be the same for each time.[21] Therefore, if controlled properly, micron particles with uniform size can be prepared by electrostatic spraying.

In electro-spray process, the micro-column outlet of precursor solution is connected to an electrospray needle through a pump, and the effluent is electro-spray to produce dry particles with the evaporate of solvent. When the liquid meniscus at the outlet of the metal capillary is kept under a high voltage field, normally higher than 10K, the free surface of the liquid at the nozzle usually shows a stable conical shape, and its apex emits a stable micro-jet and uniformly disperses into small droplets.[22]

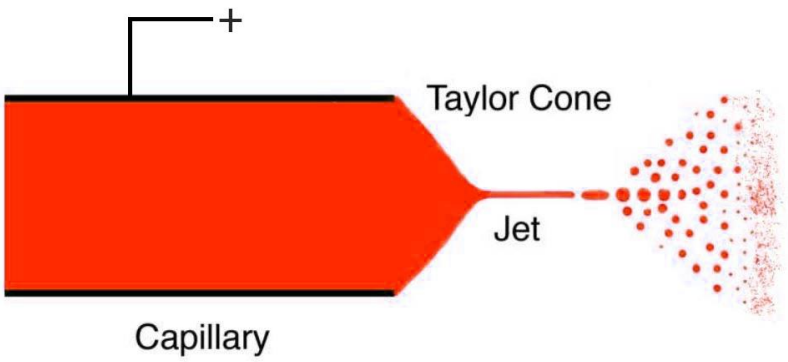

Figure1.3 Taylor cone model in electro-spray

Figure 1.3 shown the structure of Taylor cone. At the outlet of the capillary, electron concentrate on at the tip of capillary caused by tip discharged and capacity effect. The liquid phase form stable cone-shape structure jet affected by the voltage and separate into smaller evenly droplet with the collect distance increase.

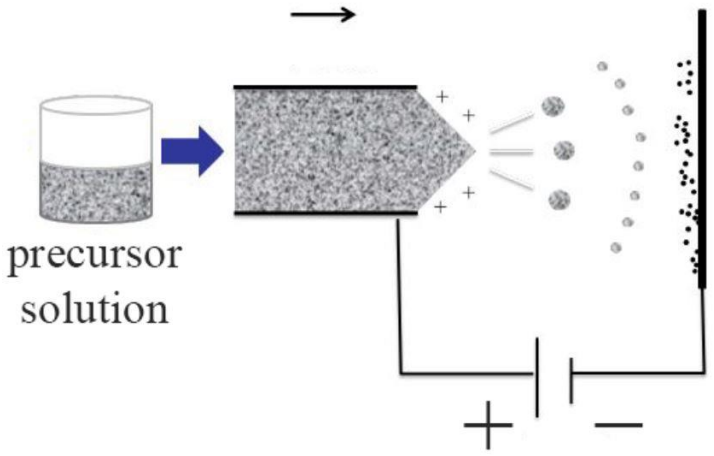

Figure 1.4 Schematic figure of electro-spray

Figure 1.4 shown the process of single wall electro-spray. As the figure shown, electro-spraying is a fast and simple process to generate core-shell structure microsphere. The precursor solution

enters the metal capillary by the force of pump and separate into small droplet under the high electrostatic field. The solvent evaporated in air and form micro- or nano- spheres collected by the negative pole such as aluminum foil or stainless iron palate.

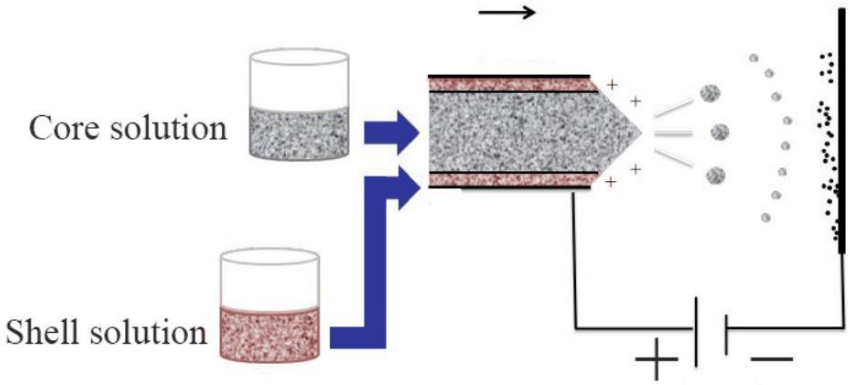

Figure 1.5 Schematic figure for co-axial electro-spray

With the develop of electro-spray, there are two type of needle for electro-spray mixture phase system: single-wall needle and double-wall needle. As the figure 1.4 and 1.5 shown above. For the first system, the solution in single needle are stable and more easily keep in one phase. Even though the concentration and proportion are more stable, we cannot make encapsulate structure based on this system. That the is the reason why we introduced the latter one: double co-axial electro-spray system in this project. As the figure M shown above, the precursor shell solution is separate with precursor core solution and be controlled by separate controller, which means that it could change injection rate and concentration separately.

Electrohydrodynamic liquid atomization (EHDA) under high voltage has been employed to generate polymer core-shell structure microspheres in recent studies. Because of the formation of electro-spinning scaffold requires only one step to fabricated, it could be termed as a micro-

processing technique. [23] According to recent studies, Berklanda et al electro-sprayed PLG (poly-(lactide-co-glycolide)) microparticles in various sizes by electro-spray process under high voltage. Meanwhile, Hong et al also reported that to generate quasi-monodisperse biodegradable polymer microparticles by separating droplets of different sizes under high voltage. [24] As studies shown, we could generate core-shell structure microsphere by electro-spray easily in one step.

In this project, we employed double wall electro-spray method to fabricated PLGA and growth factors microsphere to loading OPN (Recombinant Human Osteopontin) and SDF-1(CXCL12) in PCL scaffold at the same time to repair bond structure. A systematic study of the effect of PLGA polymer concentration and solution flow rate of growth factors on particle morphology and release result has recently been published. However, a general explanation of the processes from first principles and cells experiment are still missing.

1.4 Electro-spinning Method

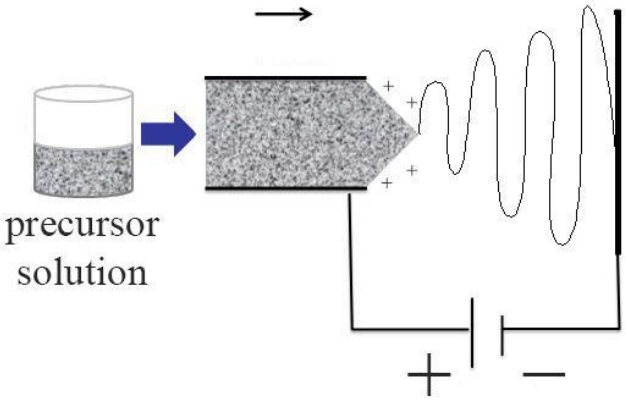

Figure 1.6 Schematic figure for electro-spinning

Electrospinning is a special form of electrostatic atomization of polymer fluids under high voltage. Electro-spinning is similar with electro-spray but in different voltage range. At this time, the material split out by atomization is not tiny droplets, but tiny polymer jets, which can run for a long distance and finally solidify into fibers. [26] It has aroused widespread interest in tissue regeneration engineering and drug delivery due to its relative ease of fabricating condition and adaptability in biomaterials. In the field of biomedicine, the diameter of nanofibers is smaller than that of cells, which can simulate the structure and biological functions of natural extracellular matrix. Most human tissues and organs are similar in form and structure to nanofibers. This is the use of nanofibers in tissues and tissues. The repair of organs offers the possibility; some electro-spinning polymer materials have good biocompatibility and degradability, which can enter the human body as a carrier for drug delivery and can be easily absorbed in human body. Also, electro-spinning nano fibers have a large specific surface area, porosity and other excellent characteristics. [27] Therefore, it has attracted continuous attention of researchers in the field of biomedicine, and has been well applied in drug release, wound repair, biological tissue engineering and other aspects. This technique is remarkably simple for control and easy to fabricate fibers with diameters ranging from nanoscale to microscale. Compare with other scaffold making method, the inherently high surface to volume ratio and high orientation property of electro-spun polymer fibers can improve cell attachment in fiber and high open porous rate, enhance drug loading efficiency, and control the rate of drug release in vivo and in vitro. Also, because of the various parameters of electro-spinning could be adjusted, the drug release profile and the degradation rate could be controlled easily compare with other scaffold generation method. Many natural and synthesis polymer has been researched for electro-spinning

fibers in recent studies. Such as collagen and PLA.[6] But the degradation of this kind of polymer is too fast for bone regeneration. Scaffolds for engineered tissues should ideally match the material that is biodegradable and non-toxic, also have mechanical properties that are match the tissue it is replacing, in this case bone tissue regeneration is the main goal for us, and support cell attachment and cell proliferations and migration. Therefore, electro-spinning is a suitable method to fabricate the PCL scaffold for bone regeneration in this study. PCL is extensively studied for controlled drug delivery. As we known, Polycaprolactone (PCL) is a bioresorbable synthetic polymer, which has been approved by the Food and Drug Administration (FDA) for the use of numerous medical and drug delivery methods. Due to the compatibility with a wide range of drugs and good mechanical properties of PCL, it has results in low cell adhesion and proliferation ability of cells. Also, due to the degradation rate of PCL is relative low compare with common natural polymer, it is suitable material for bone regeneration structural scaffold.

The figure 1.6 shown the injection model of single axial electro-spinning. As you can observed, compare with electro-spray, with the evaporation of solvent at the outlet of needle, the polymer formed linear fibers but not separate into spheres under high voltage, which is caused by the control of voltage and polymer concentration.

In this work, for the second chapter, we employed electro-spinning and electro-spray method simultaneously under different voltage to fabricate PCL scaffold with growth factors in PLGA coating microspheres to stimulate blood vessel regeneration in fracture union. In the third chapter, we employed electro-spinning method to capture ADSCs inside the PCL scaffold fabricating 3D scaffold structure for improving bone tissue regeneration.

1.5 Cell Proliferation and Migration

1.5.1 Cells for Experiment

Adipose Tissue-derived Stem Cell (ADSC) are human adult stem cells isolated from fat tissues during procedures such as liposuction, abdominoplasty, or breast reduction and can be used to promote skin and hair growth. Human Umbilical Vein Cells (HUVEC) are cells derived from the endothelium of veins from the umbilical cord. They are used as a laboratory model system for the study of the function and pathology of endothelial cells. They are used due to their low cost, and simple techniques for isolating them from umbilical cords, which are normally resected after childbirth. In this project, we employed ADSCs and HUVECs did cells proliferation and migration to explore the effective of OPN and CXCL12.

1.5.2 Cell Proliferation

With the treatment of growth factors, cells tend to increase proliferation rate. Osteopontin (OPN) is a matricellular protein that mediates diverse biological functions. OPN is involved in normal physiological processes and is implicated in the pathogenesis of a variety of disease states. SDF-1, also known as CXCL12, is a kind of classical chemotactic agent, which is expressed by human gingival fibroblasts and periodontal ligament fibroblasts. As a growth factor, SDF-1 and its receptor, C-X-C motif receptor 4 (CXCR4) play a vital role in the development of embryonic organs, maintaining tissue homeostasis after birth and bone remodeling. [28]

1.5.3 Cells Migration

Collagen is a major constituent of the extracellular matrix in vivo and collagen substrata in vitro. Collagen gel not only play an important role in vivo, but also control cell proliferation and migration in vitro experiment. [29] In this case, we estimate the function of growth factors by doing migration on collagen gel and quantify the migration distance by confocal fluorescence confocal microscopy. We not only did the migration on collagen gel, not also did migration on PCL scaffold with growth factors directly.

1.6 Mechanical Property

As we knew, PCL scaffold is a low degradation rate bioresorbable synthetic polymer. The property of PCL scaffold we fabricated should match the mechanical property for bone tissue. In this research, we employed single axis tensile test to explore the Yang's module and ultimate elongation rate for PCL scaffold.

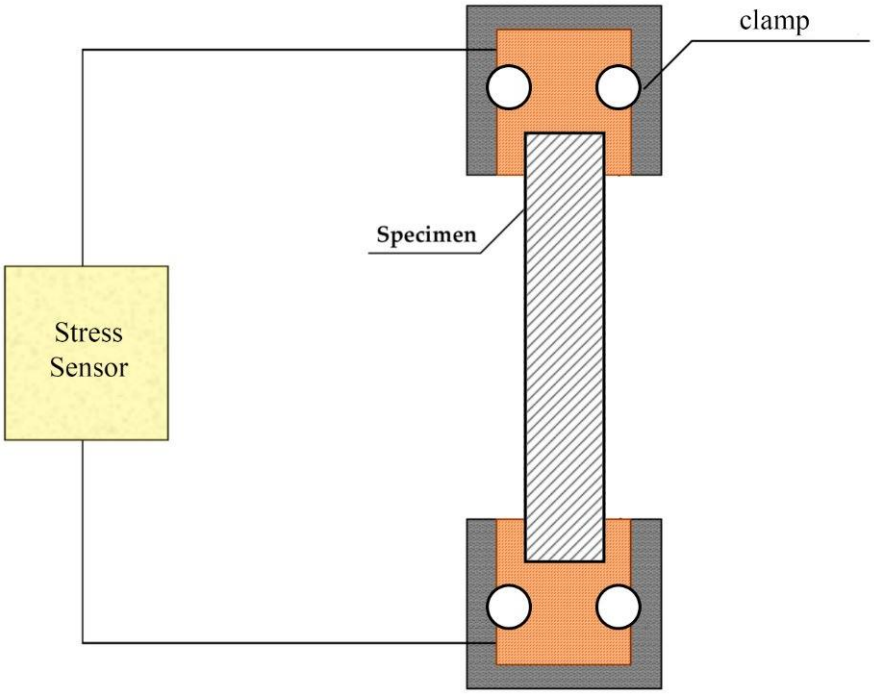

Figure 1.7 Schematic figure for tensile test machine

As figure 1.7 shown, the two clamps stretch into opposite direction and the sensor collect the data for current stress. With the extension of one clamp, data of stress and moving distance were collected by sensor.

Chapter 2: Fabricating Growth Factors Microspheres in Fibrous Scaffold

2.1 Methods

2.1.1 Preparation for Precursor Solution

For all the materials used in experiments to fabricate scaffold with growth factors are listing below. Poly(lactide-co-glycolide) (PLGA, LA/GA 50:50, in DCM, SIGMA-Aldrich), polycaprolactone (PCL, MW70−90 kDa, Sigma-Aldrich), chloroform (CHCl3, SIGMA-Aldrich), dimethylene chloride (Sigma-Aldrich), gelatin (type B, SIGMA-Aldrich), Hoechst (Invitrogen), rhodamine B base (Sigma-Aldrich), SDF-1a(CXCL12)(Peprotech), and Recombinant Human Osteopontin (OPN) (Peprotech).

The PLGA solution and the growth factors solution were introduced into the outer and inner tubing, respectively. For preparing PLGA solution for shell structure, the PLGA solution in methylene chloride had a concentration of 5 wt % and shake until fully dissolved. The preparation process of core solution is the next step. Dissolve 0.5wt% gelatin B in PBS solution in advance until not chuck inside the solution. Then dissolve 20ug CXCL12 and 100ug OPN in 1ml gelatin B/ PBS solution to form electro-spray precursor solution and storing in -20℃ for keeping bioreactivity. Dissolved 10wt% PCL (polycaprolactone) in chloroform and shacked until into one phase for precursor of electro-spinning solution.

The samples for confocal microscope are prepared in same way but included staining materials for showing the structure of capsule structure. For the core solution, we replaced growth factors into BSA because of economic reason and staining by 50um/ml Hoechst to combined with BSA for showing the fluorescence signal. In the shell solution, we introduced rhodamine B base for staining PLGA, the concentration for rhodamine B base was 10ug/ml in shell precursor solution. The fluorescence signal was captured by Zeiss confocal fluorescence microscopy.

2.1.2 Scaffold Fabricating Process

The OPN and SDF-1 α -encapsulated PLGA microspheres were fabricated via coaxial electro-spraying and the PCL scaffold were fabricated by single coaxial electro-spinning simultaneously. The coaxial needle and structure shown in Figure 2.1. The inner diameter of co-axial is 0.70mm and the outlet diameter of co-axial is 1.65mm for electro-spray.

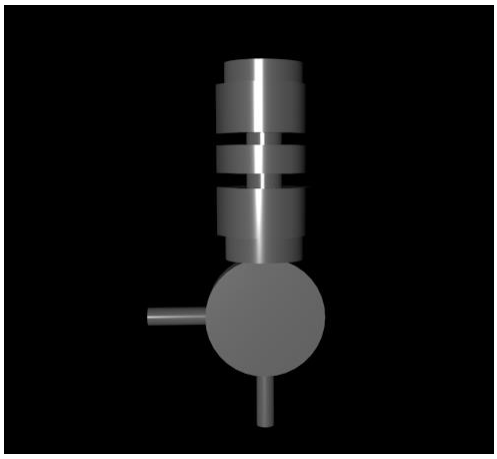

Figure 2.1 co-axial electro-spray needle 3D model

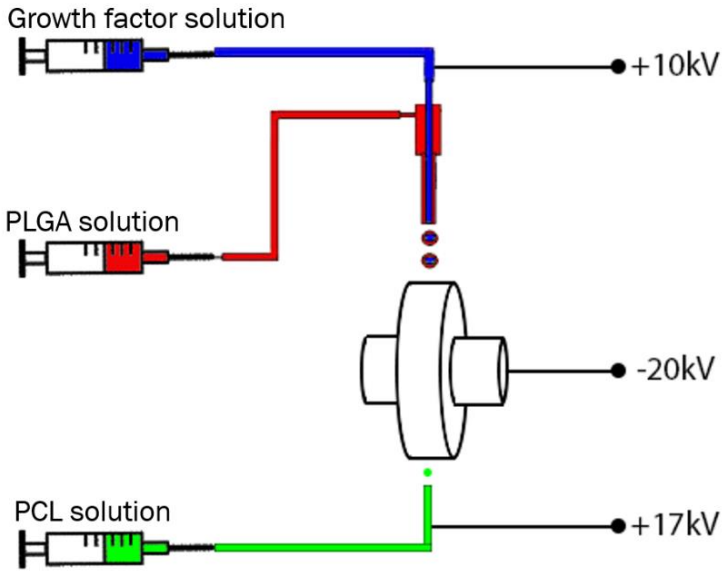

Figure 2.2 schemaic figure for PCL scaffold fabricated process

Two growth factors solutions (in PBS) with concentrations of 20ug/ml for SDF-1 and 100 μg/ mL for OPN containing 0.5 wt % of gelatin to increase the viscosity of the solution during electro-spraying process and offer structural support for microsphere after the evaporation of organic solutions. The SDF-1a and OPN solution was injected into the inner tube inside the electro-spray needle through syringe by pump A, as the blue part in figure 2.2 shown, via an injection rate 0.5 mL/h. Whereas the PLGA solution was injected into the outlet tube through syringe by pump B, as the red part in figure 2.2 shown via an injection rate of 1 mL/h. The coaxial needle and collecting mandrel were charged at +20 and −10 kV by high voltage generator respectively. The mandrel connected to the ground. The 10wt% PCL/chloroform solution were injected through syringe by pump C to electro-spinning needle forming PCL fiber under high voltage. The injection rate was 5ml/h and the statistic voltage were +17kV. The diameter of collector, which was a collecting mandrel in this case is 13cm and the injection rate

is 800rpm. The distance between electro-spray needle and the collector are 30cm, the distance between electro-spinning needle and the collector is 20cm.We assumed the collecting mandrel could separate electron evenly on the aluminum foil surface and no electron-arc generated in ideal situation. Humidity of the atmosphere were keeping in 80% and temperature was keeping in room temperature (25℃) all the time. The process of fabricated took 45 minutes per PCL scaffold. After fabrication, the fabricated microspheres with fibers were vacuum-dried overnight to remove residual solvent and stored at −20 °C for keeping bioreactivity for further experiment.

2.1.3 Characterization

The microspheres samples collected during the process of electro-spray by slide glass mounting with CC mount and covered with glass for short term storage. The distance of collecting is same with the drum collector for fabricating PCL scaffold. Image of the microspheres were obtained with a Zeiss 510 META laser scanning confocal microscope. The laser frequency for Hoechst is 350/461 nm and laser frequency for rhodamine B base is 544nm. The resolution for florescence capture image is 1920*1920 pixels. The figures did post processed and edited by image J software.

The structure of scaffold with microsphere were shown by SEM image. After the process of vacuum-dried, with sputter gold coated to increase conductivity, and observed under SEM at an acceleration voltage of 5kV to characterize the morphology of the scaffolds with microspheres.

2.1.4 Release for growth factors in vitro

The scaffolds with OPN and SDF-1a growth factors were cut into pieces (50 mg/piece) and placed into 1 mL centrifuge tubes with 5 repeats for different types of scaffolds. PBS (pH 7.4)

supplemented solution with 1% penicillin for antibacterial was used as a release medium for OPN and SDF-1a. The release study was conducted at stable 37 °C water bath. For scaffold only included SDF-1a or BSP, collected samples and quantify growth factor concentration with matching ELISA kit. For scaffold included both BSP and SDF-1a, quantify both concentration of growth factors separately by ELISA kits. The release medium was collected at predetermined time intervals during the 28-day period at each collecting time point designed previously (1/3/5/7/14/21/28 days), and 1 mL of fresh release medium was then added to each tube each time point for replacement. The concentration of OPN and SDF-1a in the collected release medium was determined by a BSP ELISA kit (Peprotech Cooperation) and SDF-1a ELISA kit (Peprotech Cooperation). With the data of growth factors released in each sample in 5 repeats, the BSP and SDF-1a release curve could been calculated and compared with theorical value.

2.1.5 Tensile Test

The PCL scaffold was cut into rectangle shape for tensile test. The thickness of the fabricated scaffold was 150um, the length is 15 mm, and the wide of the scaffold was 1 mm with 3 repeats sample. We tested the Young's module for direction parallel with collector rotation direction which is the fiber-prefer direction.

2.1.6 Cells Migration

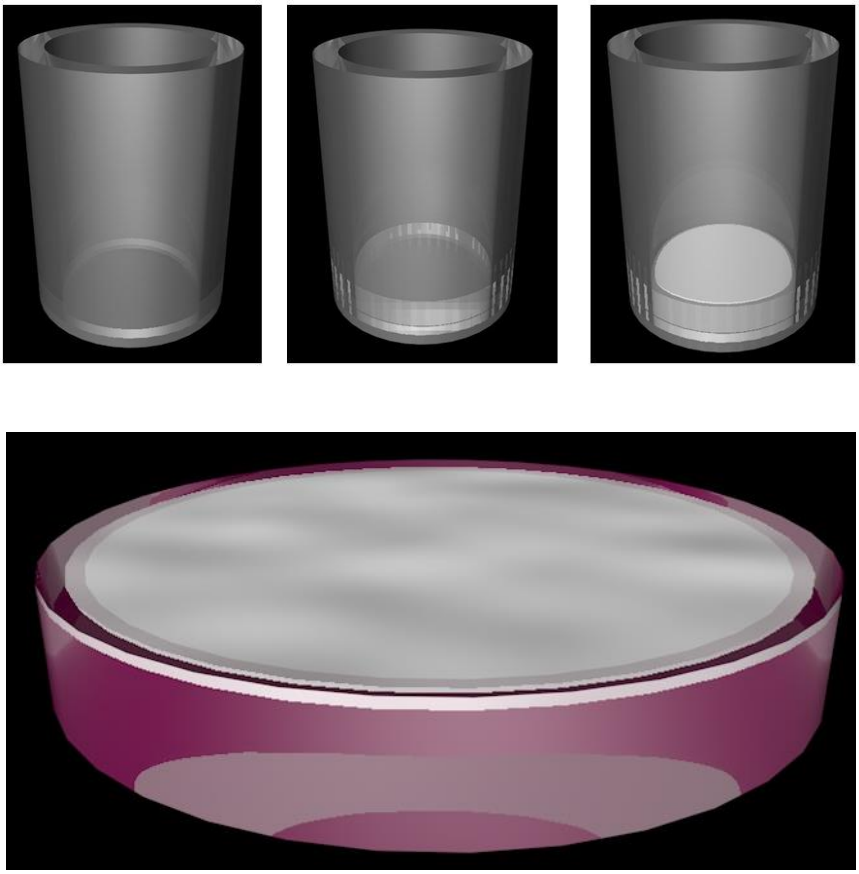

figure 2.3 coating model for PCL scaffold

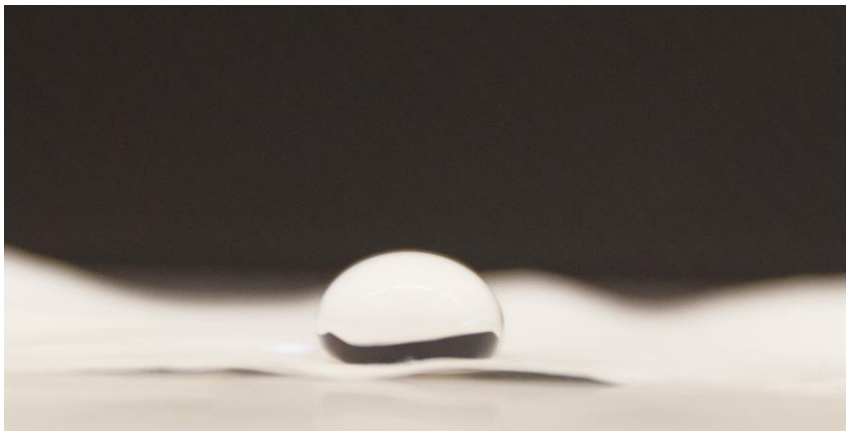

figure 2.4 contact angle of PCL scaffold

Bioactivity of the OPN and SDF-1microspheres in fabricated PCL scaffolds was further evaluated for its ability to support cells migration on collagen gel and on the PCL scaffolds. As the figure 2.4 shown above, the contact angle for water is higher than 90 degree, which proved that the PCL scaffold are hydrophobicity, also the density of the scaffold is far much smaller than water. As a result, the fabricated PCL scaffold will be floating on the culture medium in cell experiment without any treatment. For cells migration on surface of the PCL scaffold, we came out a solution to solve this problem by coating scaffold to the bottom of the 96-well with agarose gel. Before experiment, the scaffolds with proteins were punched into 6 mm disks by punch for keep in same volume and sterilized under UV light for 1 h in the laminar flow hood, stored the 4 types of scaffold in -20℃ for keeping bioactivity. As the figure 2.4 shown above, the PCL scaffold was fixed on the bottom of the well by agarose gel. The process for coating is introduced below. Firstly, dissolve agarose (1.5wt%) in PBS solution in glass bottle by heat it up in microwave oven until fully dissolved in one phase and transparency. Keep the glass bottle in hot water preventing cool down too quickly and set to solid gel in coating progression. Then coating the 96-well plate and put scaffold on top immediately after dipping one drop of agarose solution on the bottom of well to make sure scaffold stick on agarose gel before the gel was totally set to solid. After coating all the scaffolds sample, sterilizing the 96-well plate with scaffold for further experiments.

The HUVECs were cultured in F-12K Medium (Kaighn's Modification of Ham's F-12 Medium) with 10%FBS(Thermo fisher) and 5 mL endothelial cell growth supplement (ECGS; BD Biosciences catalog # 354006) for 500ml medium. HUVECs were suspended in culture medium,

density of cells is 0.1M/ml with treatment of iL1-beta, then loaded 300ml cell suspension solvent into each well in 48-well plate. s

The ADSCs were cultured in MEMa with 10%FBS and 1% Pen. The structure of PCL scaffold with agarose gel shown in figure 2.4, the pink transparent gel is agarose and the white membrane is PCL scaffold. The seeded PCL scaffolds on agarose gel and on collagen gel were incubated under 20% O2 and 5% CO2 in sterile incubator. After 1 day, 3 days and 7 days of culture on scaffold and 2 days on collagen gel, the PCL scaffolds were collected and fixed with 4% paraformaldehyde solution for further characterization. Cells in collagen gels and scaffold were imaged by confocal microscope and processed by image J. To quantify cell migration, we counted cells number at every 10 μm at vertical direction for the entire migration section.

2.1.7 Cells proliferation

Before experiment, the scaffolds with proteins were punched into 6 mm disks by punch and sterilized under UV light for 1 h in the laminar flow hood, stored the 4 types of scaffold in -20℃ for keeping bioactivity for further experiments. Dissolve agarose (1.5wt%) in PBS solution in glass bottle by heat it up in microwave oven until fully dissolved in one phase and transparency. Keep the glass bottle in hot water preventing cool down too quickly and set to solid gel in coating progression. Then coating the 96-well plate and put scaffold on top immediately after dipping one drop of agarose solution on the bottom of well to make sure scaffold stick on agarose gel before the gel was totally set to solid. After coating all the scaffolds sample, sterilizing the 96-well plate with scaffold for further experiments. For the samples in 96-well plates, Adipose Tissue-derived Stem Cell (ADSC) were cultured on the PCL scaffold surface at a cell density of 1 × 105 cells/mL with 3 repeats for each samples and time points. For the

fabricated PCL scaffolds, the seeded scaffolds were incubated under 20% O2 and 5% CO2. After 1 day, 2 days and 7 days of culture, the scaffolds were collected and tested DNA amount by DsDNA test kit. And Detected florescence single by confocal florescence microscopy with the process of image J.

2.1.8 In vivo Experiment

With the Cooperated from Professor Shen at School of Medicine at Washington University in St. Louis. The scaffolds were implanted into RA mice with bone fracture.

2.2 Characteristic result

2.2.1 Confocal florescence microscopy image

Core-shell microsphere was fabricated through electro-spray as previously described. As the figure 2.5 shown above, the green florescence generated by Hoechst showing the structure of core and red florescence generated by Rhodamine B base showing the structure of shell. The center of the shell are empty based on the florescence single shown in figure, which can prove that PLGA form coating outside the gelatin and growth factors.

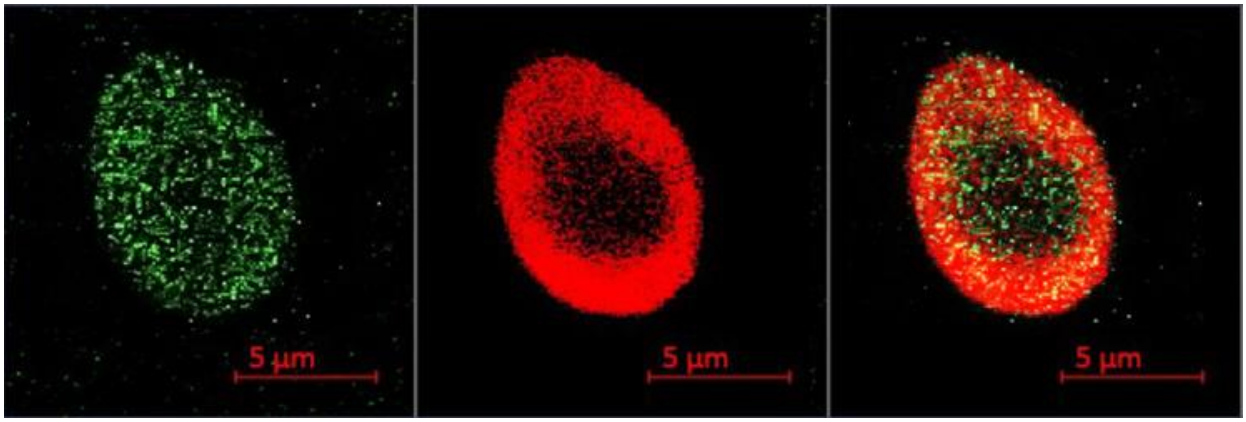

Figure 2.5 Confocal Fluorescence Microscopy image for microspheres

2.2.2 SEM image

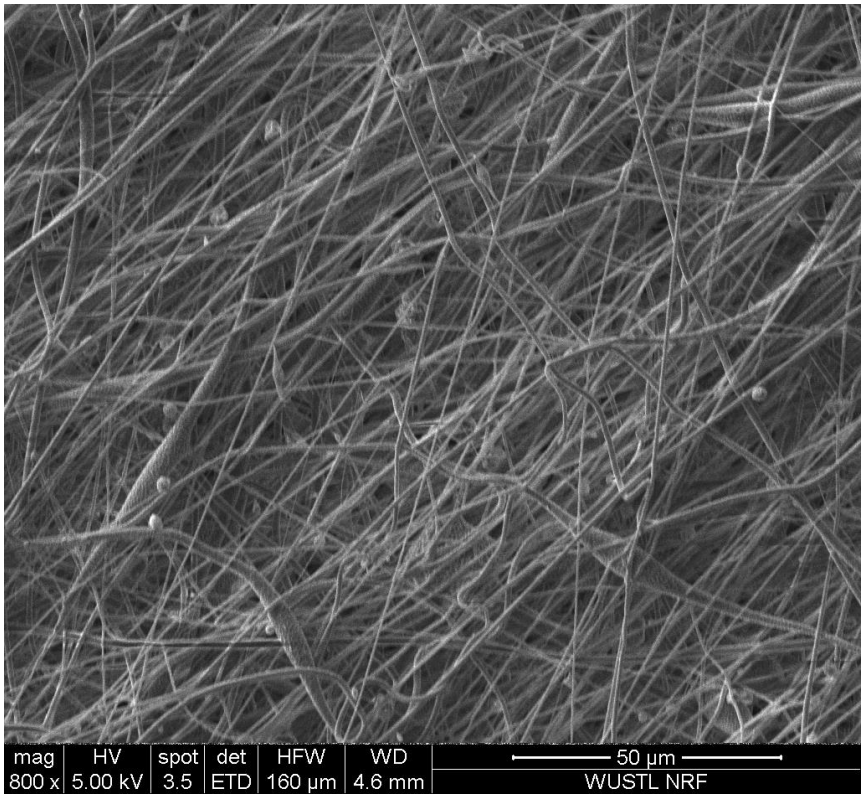

Figure2.6 A SEM image of PCL scaffold with microsphere

Figure 2.6 B SEM image of PCL scaffold with microsphere

The figure 2.7A and 2.7B are the morphology of PCL scaffold with growth factors microspheres via electro-spinning and electro-spray detected by SEM. The fibers appeared smooth and uniform and no bead was found on the fibers. The diameter of the PCL fiber is around 1 micrometer. The orientation of fiber can be observed from figure 2.7A. Majority of fiber stretch to upper right in SEM image, suggesting that PCL membrane may act as an effective carrier for microspheres. For microsphere, the diameter of microsphere is around 5 micrometers as shown in the figure, which is matched with image from confocal florescence microscope. Also, the microspheres are not only shown on the surface of the scaffold not also trapped inside the PCL scaffold. Also, the size of the microspheres is uniform and evenly. The surface of microsphere is not flat and have some rankle on the surface, which might cause by air-dry process.

2.3 Mechanical Property

The scaffold was tested on single axial tensile test machine. The curve for stress-stain is shown in figure 2.8. The highest stress of electro-spinning fabricated PCL scaffold is 28.78MPa and the max elongation rate is 298%, the Young's module is 111.52MPa. Because of the flaw of fabricated scaffold, the error bar of Young's module is high. The Young's module for pure PCL is 280MPa. Compare with data of pure PCL, the data of electro-spinning is lower than pure PCL cause by porous and fibrous structure of PCL.

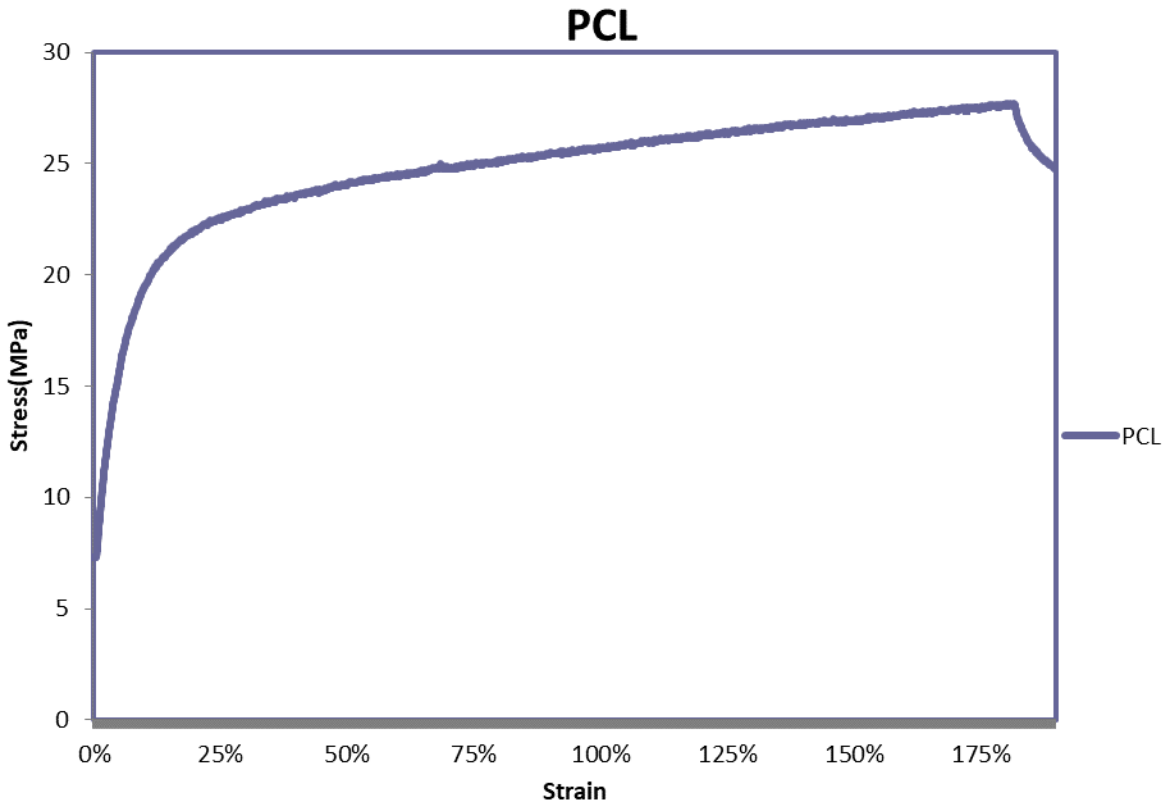

Figure 2.7 Stress-strain curve of PCL scaffold

Table2.1 Results of Tensile Test

Scaffold type	Ultimate Strength (MPa)	Young's Modulus (MPa)
PCL	28.78(±5.12)	115.52(±45.0)

2.4 Growth Factors Release

Figure 2.9A and 2.9B shown the release kinetics of bioactivity curve of OPN and CXCL12. The samples for each point was repeats with 5 times. The red curve shown the release cumulation of PCL scaffold with both OPN and CXCL12. The black curve shown the release of PCL scaffold only have OPN or only have CXCL12 inside. The cumulated OPN and CXCL12 are almost the same means that adding other protein is not e\affect the release of original protein. With the increase of time, the amount of growth factors released decrease. The max release amount is the first day in release medium based on the release curve.

The cumulated quantity of OPN is 2600pg/ml and CXCL12 is 1000pg after the end of 28 days. Based on the process of fabricated, the quantity of OPN is 45ug and CXCL12 is 7.5ug. The efficiency is around 1%. The probable reason is the rotation speed of the collector is too high to capture the microspheres.

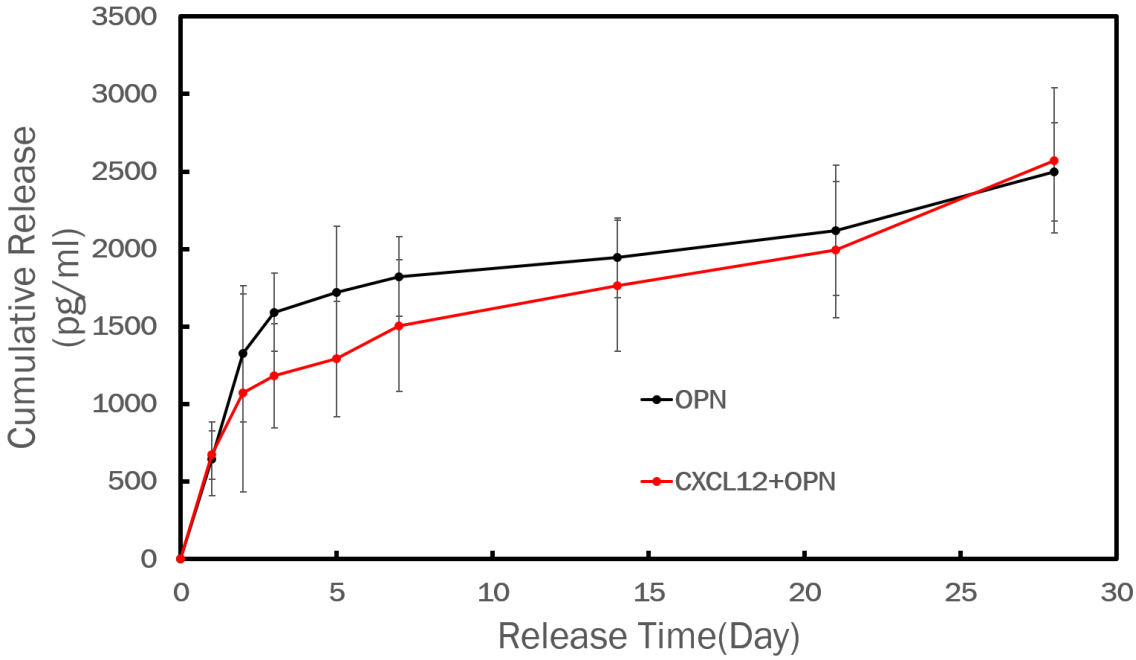

Figure 2.8A Release of OPN in microspheres

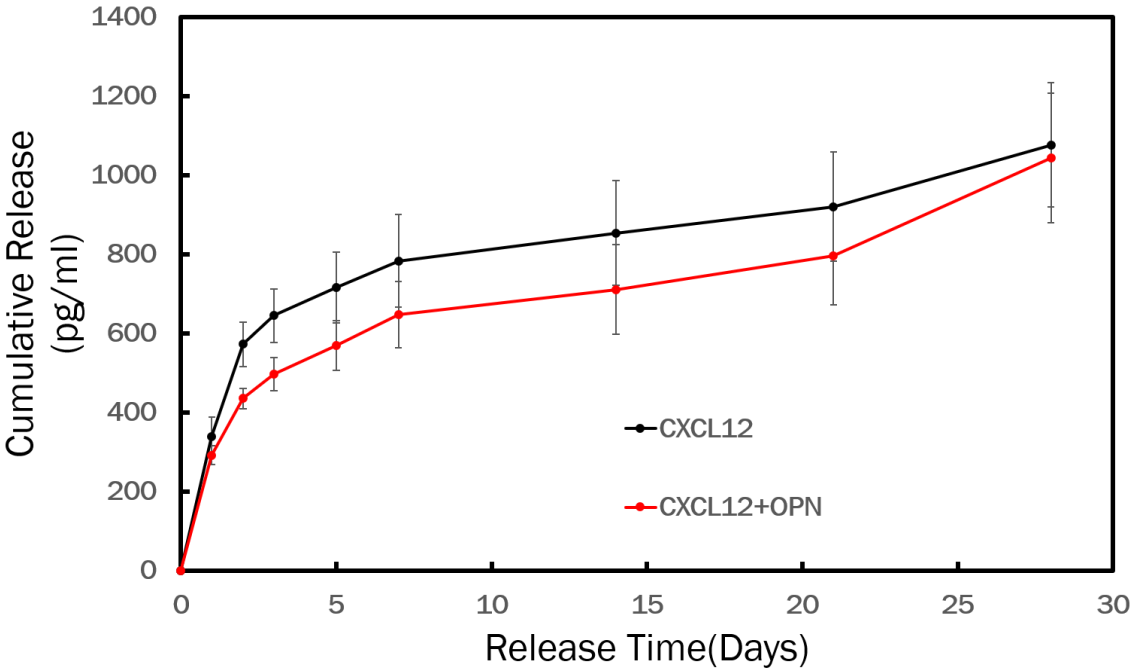

Figure 2.8B Release curve of CXCL12 in microspheres

2.5 Cell proliferation

ADSCs on scaffold with growth factors, captured GFP fluorescence in ADSCs by confocal microscope with Z-stack and tested DsDNA content in scaffold and agarose gel underneath.

2.5.1 DsDNA result

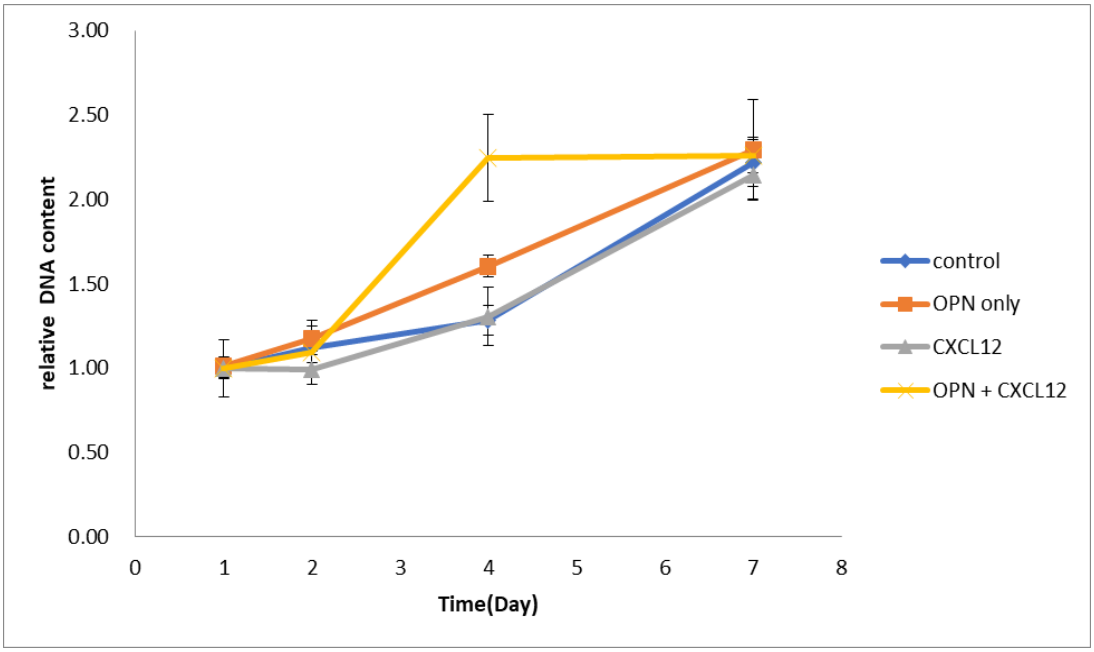

Figure 2.9 DsDNA content of cells on PCL scaffold

Figure 2.10 shown the relative DNA content of ADSCs cultured on the scaffold with growth factors treatment encapsulates microsphere. With the treatment of OPN and CXCL12, the relative DNA content increase dramatically at day 4. The DsDNA content reached the same level for four group at day 7, the probable reason is the cells number reached the maximum in the PCL scaffold after culture of 7 days.

2.5.2 Confocal Fluorescence Microscope Image

Figure 2.11 show the typical fluorescence Z-stack image of scaffold with ADSCs. We can observed that ADSCs moved into PCL scaffold during culture process based on confocal data.

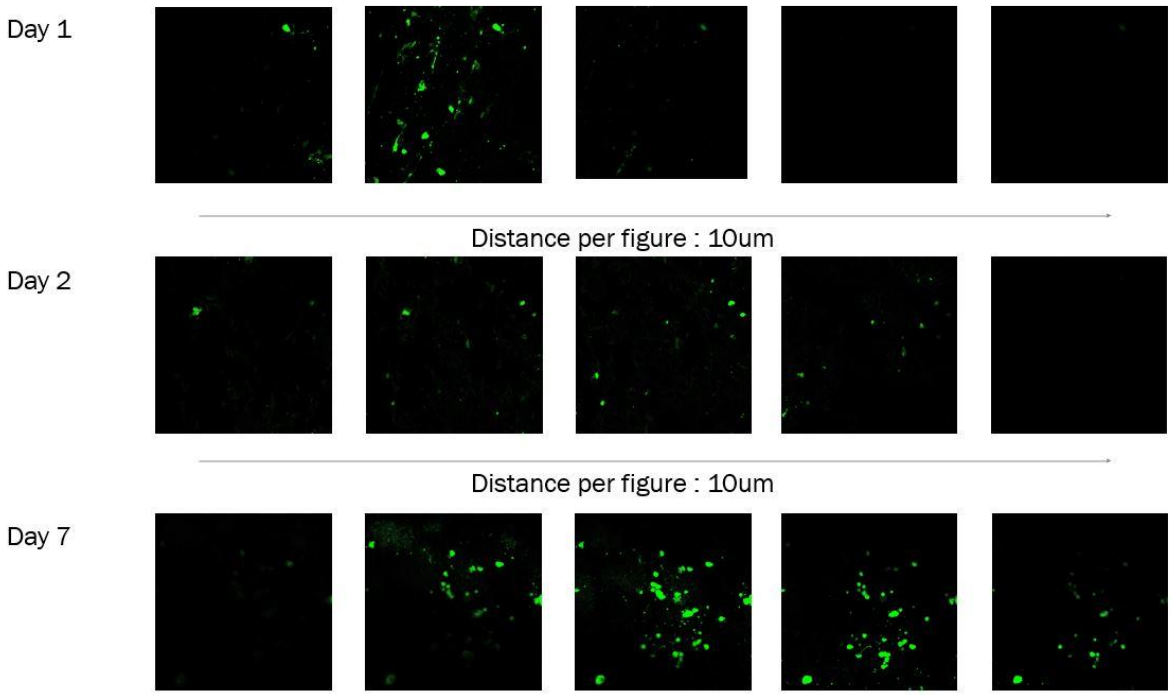

Figure 2.10A confocal fluorescence microscopy image of control group

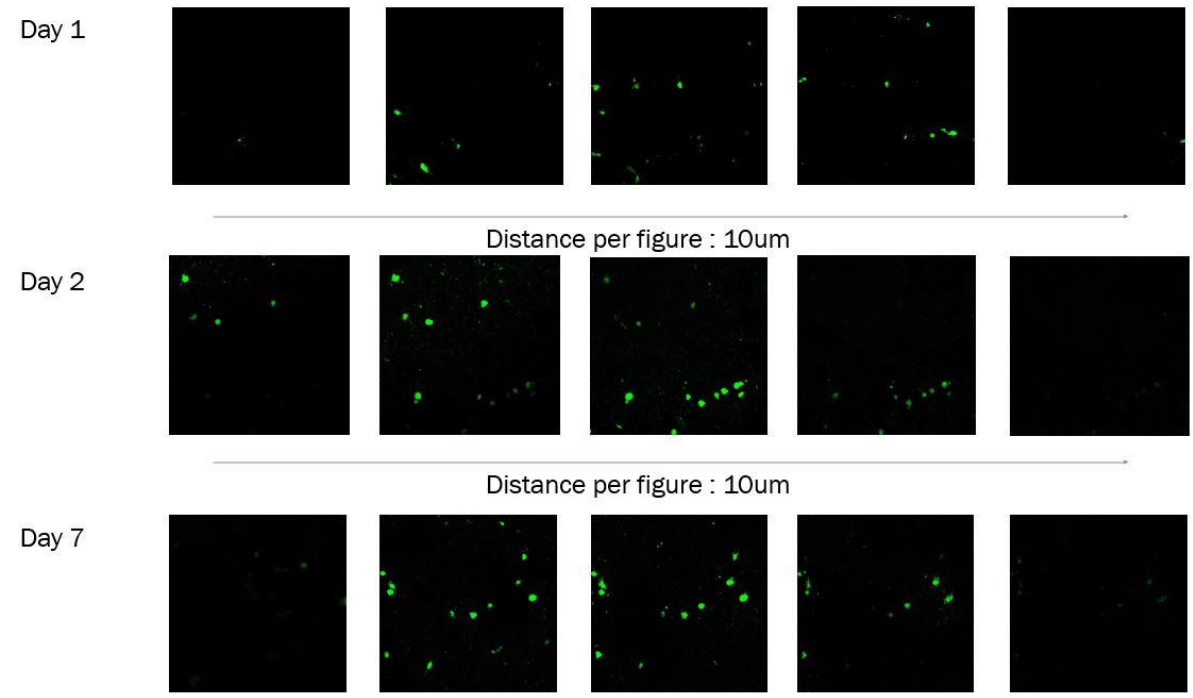

Figure 2.10B confocal fluorescence microscopy image of OPN only

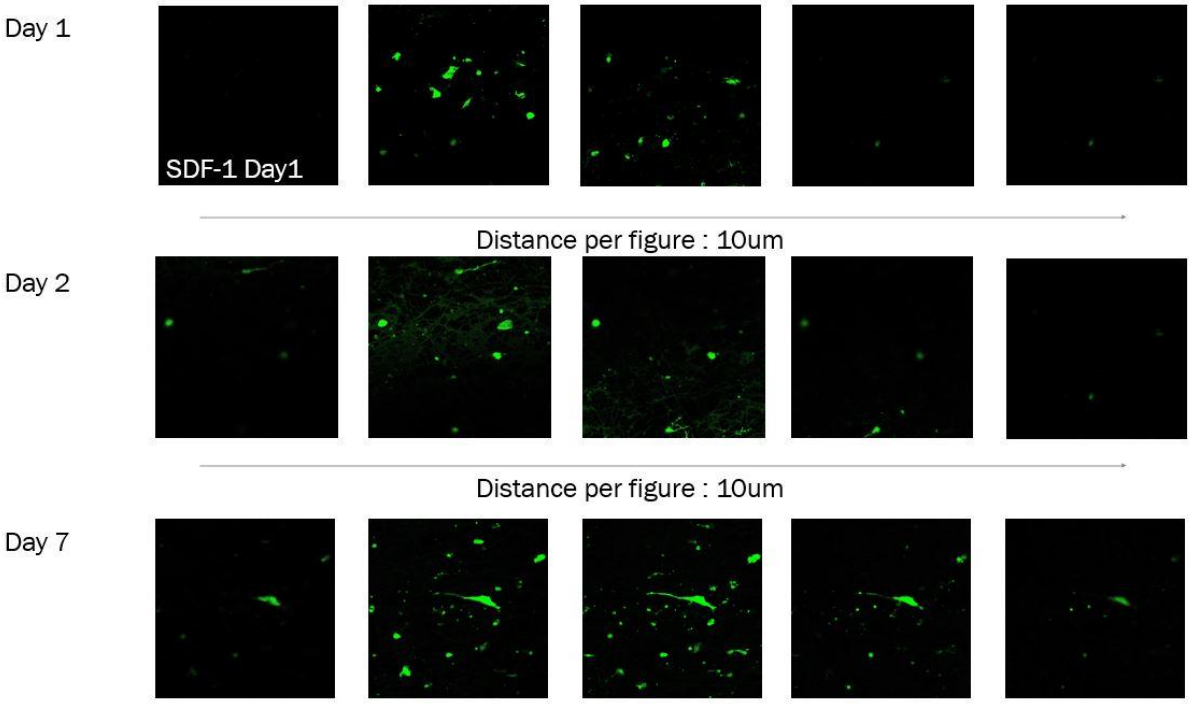

Figure 2.10C confocal fluorescence microscopy image of CXCL12 only

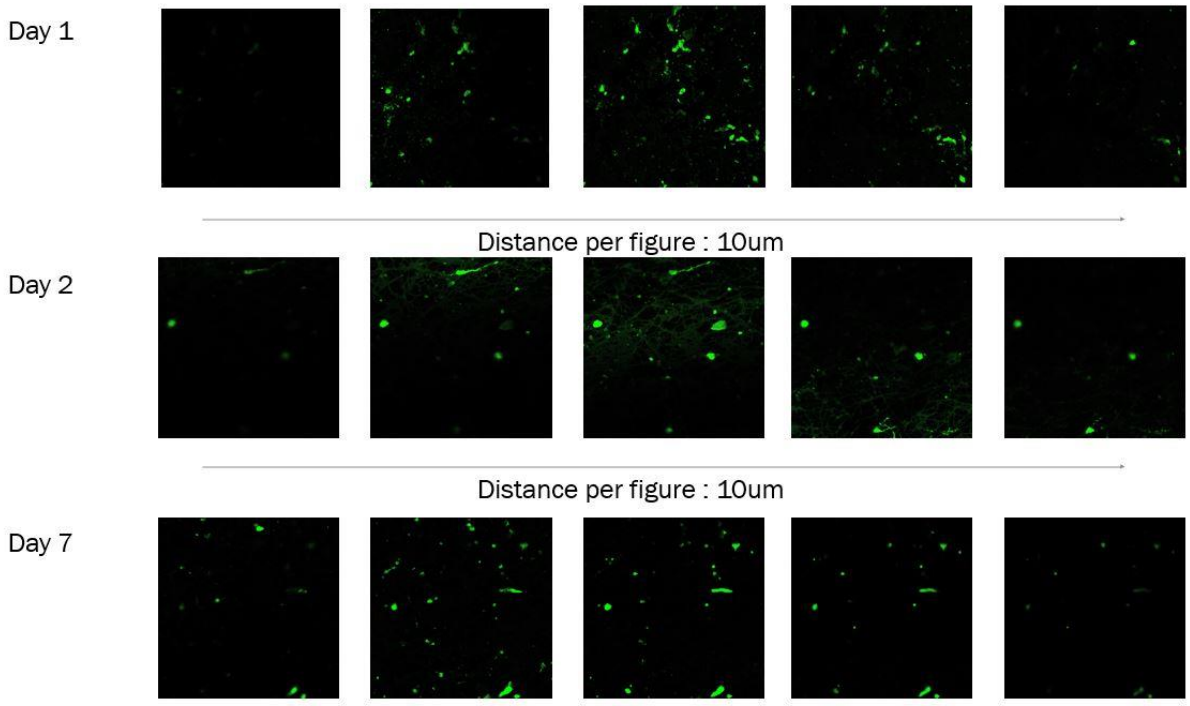

Figure 2.10D confocal fluorescence microscopy image of OPN and CXCL12

2.6 Cells migration on collagen gel

ADSCs migrated on collagen gel with Il1-beta treatment after two days. FGP signal were captured via confocal fluorescence microscopy with Z-stack and quantified migration depth of ADCSs by image J.

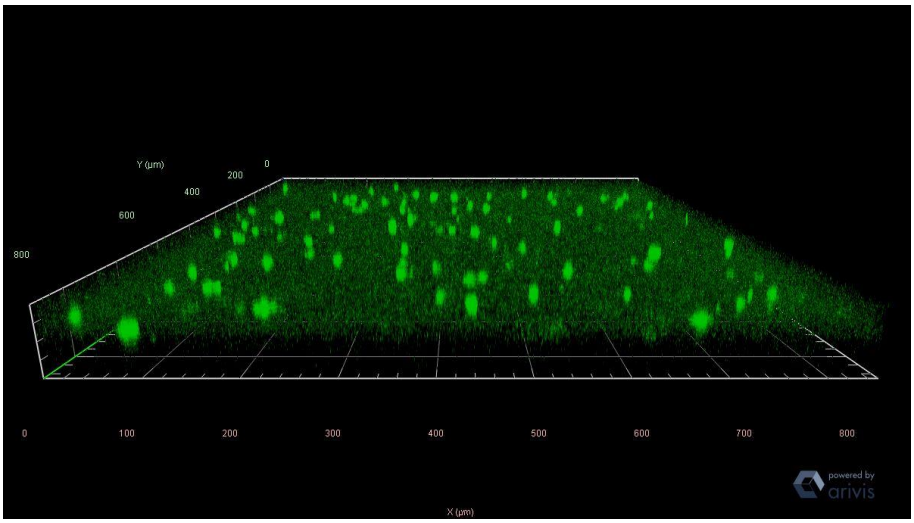

Figure 2.11A Pure PCL scaffold migration 3D image

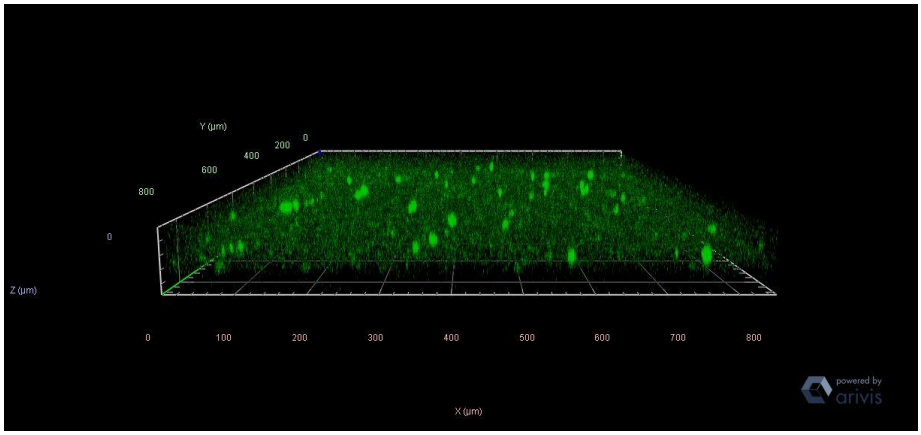

Figure 2.11B PCL scaffold with OPN microsphere migration 3D image

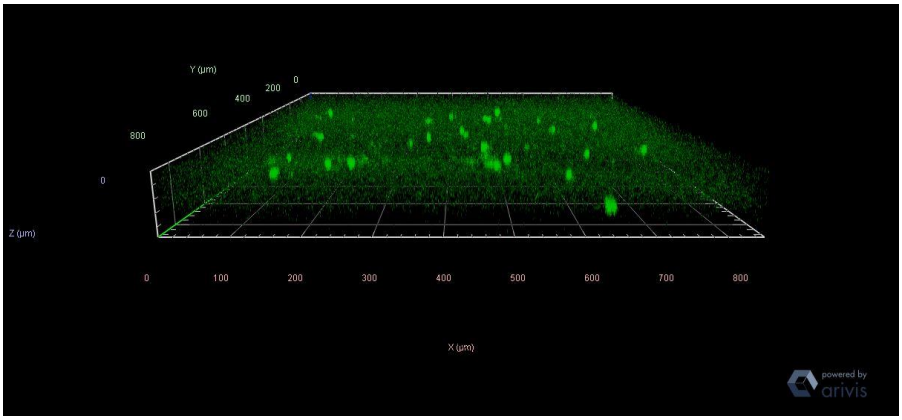

Figure 2.11C PCL scaffold with CXCL12 microsphere migration 3D image

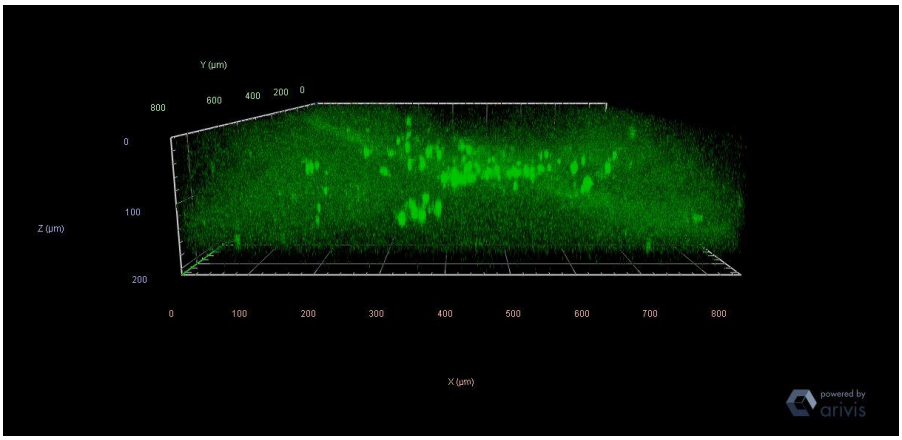

Figure 2.11D PCL scaffold with CXCL12 and OPN microsphere migration 3D image

The ADSCs cells migration in collagen gel and detect florescence single by confocal fluorescence microscope. Figure 2.12 show the typical 3D image of HUVECs migration on collagen gel of four samples based on Z-stack image. The statistic results based on Z-stack image are shown in next part.

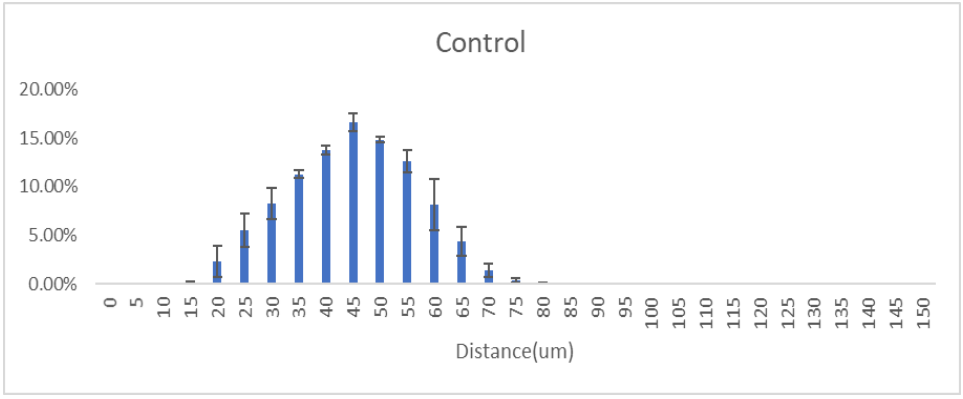

Figure 2.12A HUVECs migration distance of control group

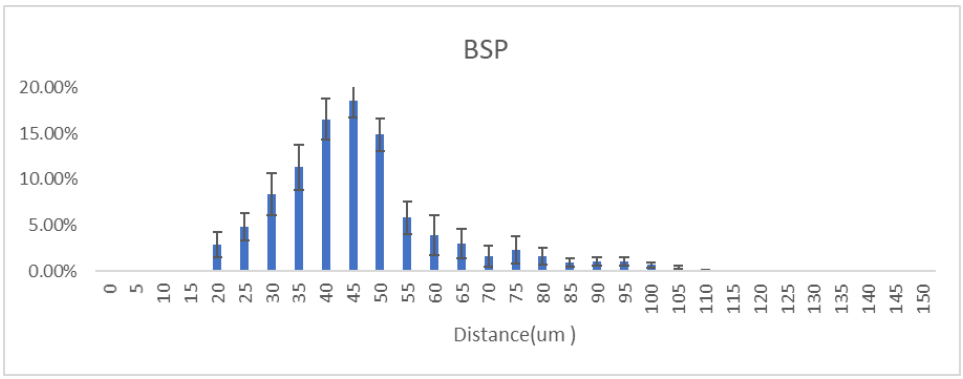

Figure 2.12B HUVECs migration distance of scaffold with OPN only

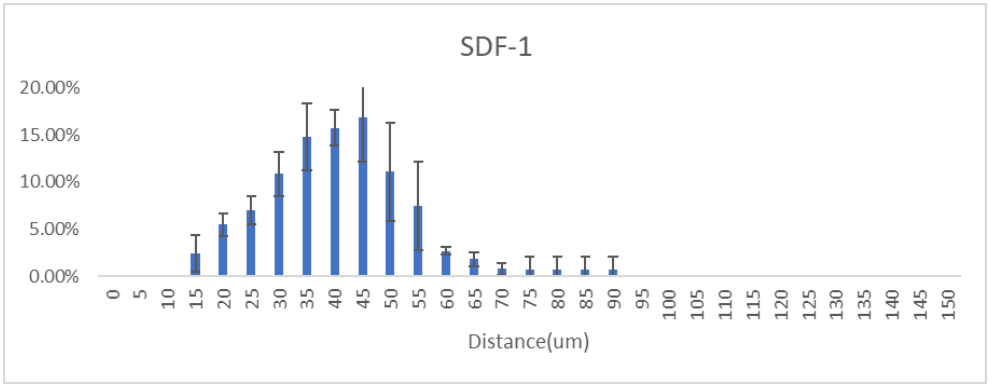

Figure 2.12C HUVECs migration distance of scaffold with CXCL12 only

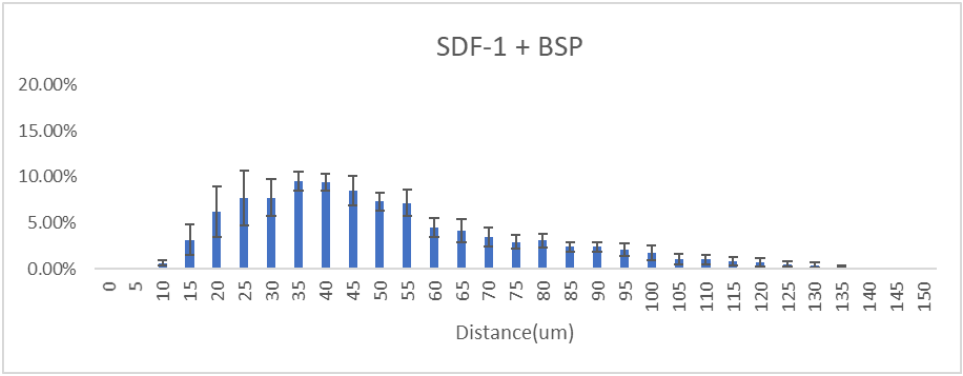

Figure 2.12D HUVECs migration distance of scaffold with OPN and CXCL12

As figure 2.13 shown above, after 2 days of culture and fixed with 4% PFA. With the treatment of OPN and CXCL12, the maximum migration distance increased. With only one growth factors treatment also could affect the migration distance but not as much effective as both.

2.7 Cell migration on scaffold

2.7.1 Confocal Fluorescence Microscopy Results

Figure 2.13A Typical Z-stack Fluorenes image for migration control group

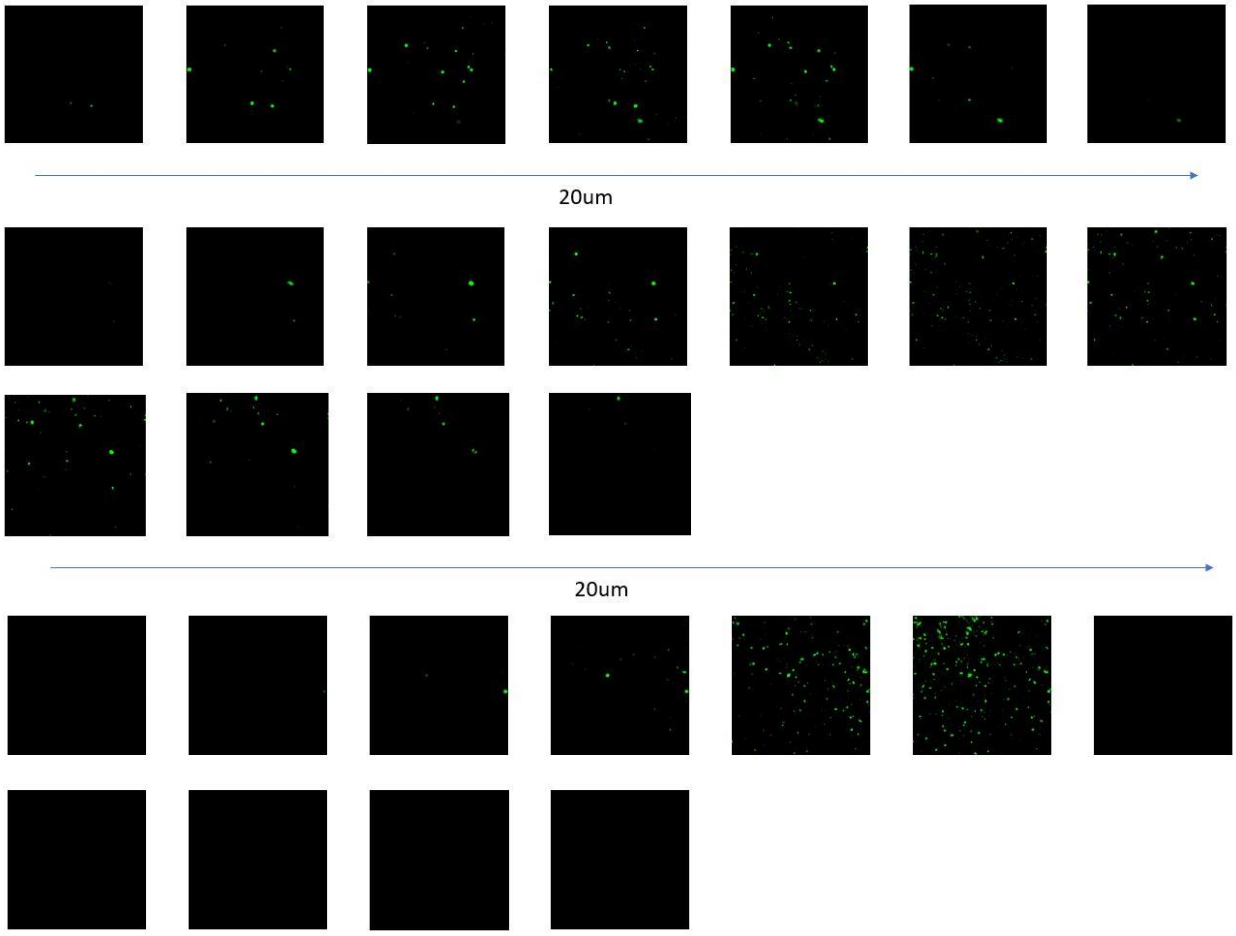

Figure 2.13B Typical Z-stack Fluorenes image for migration with OPN only

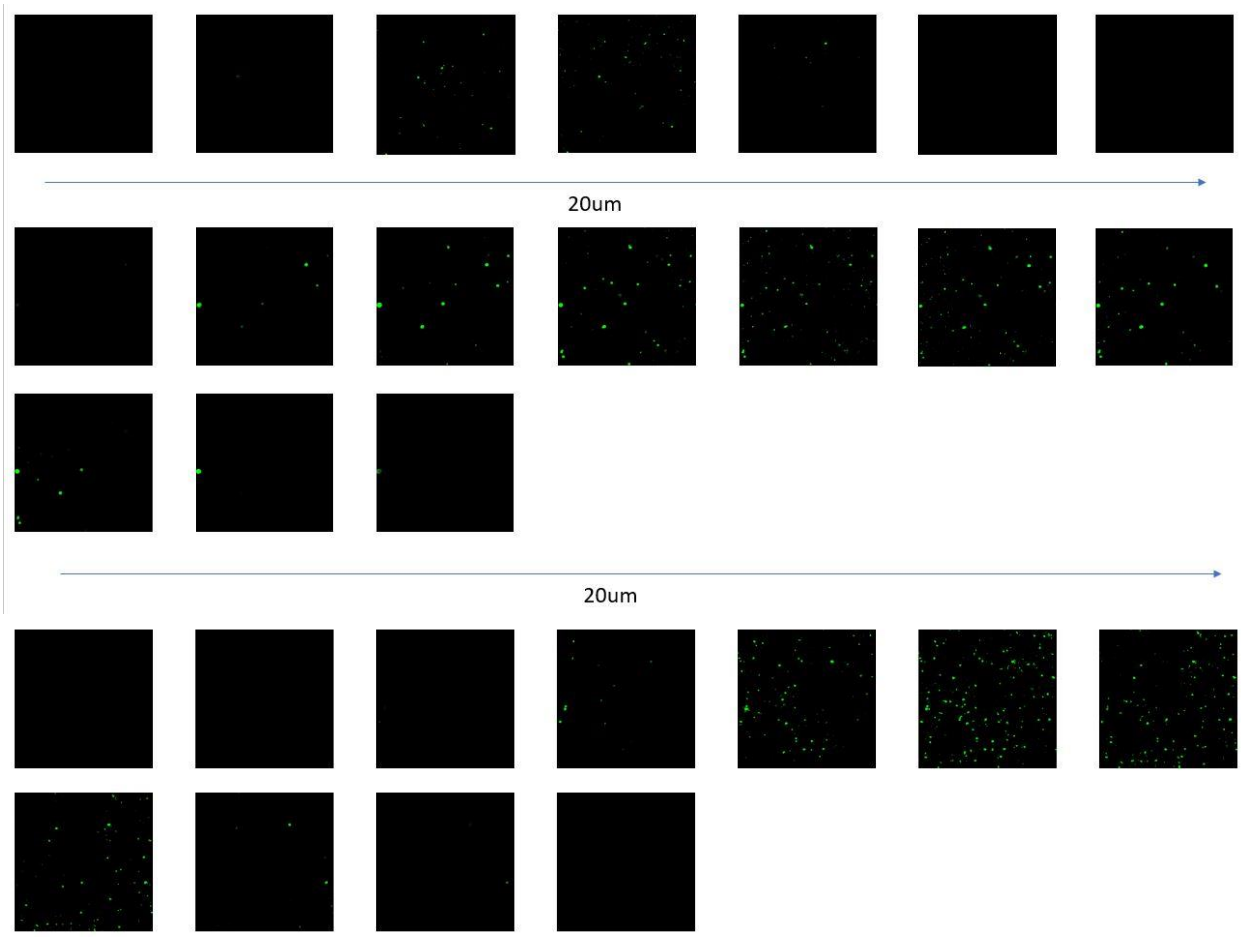

Figure 2.13C Typical Z-stack Fluorenes image for migration with CXCL12 only

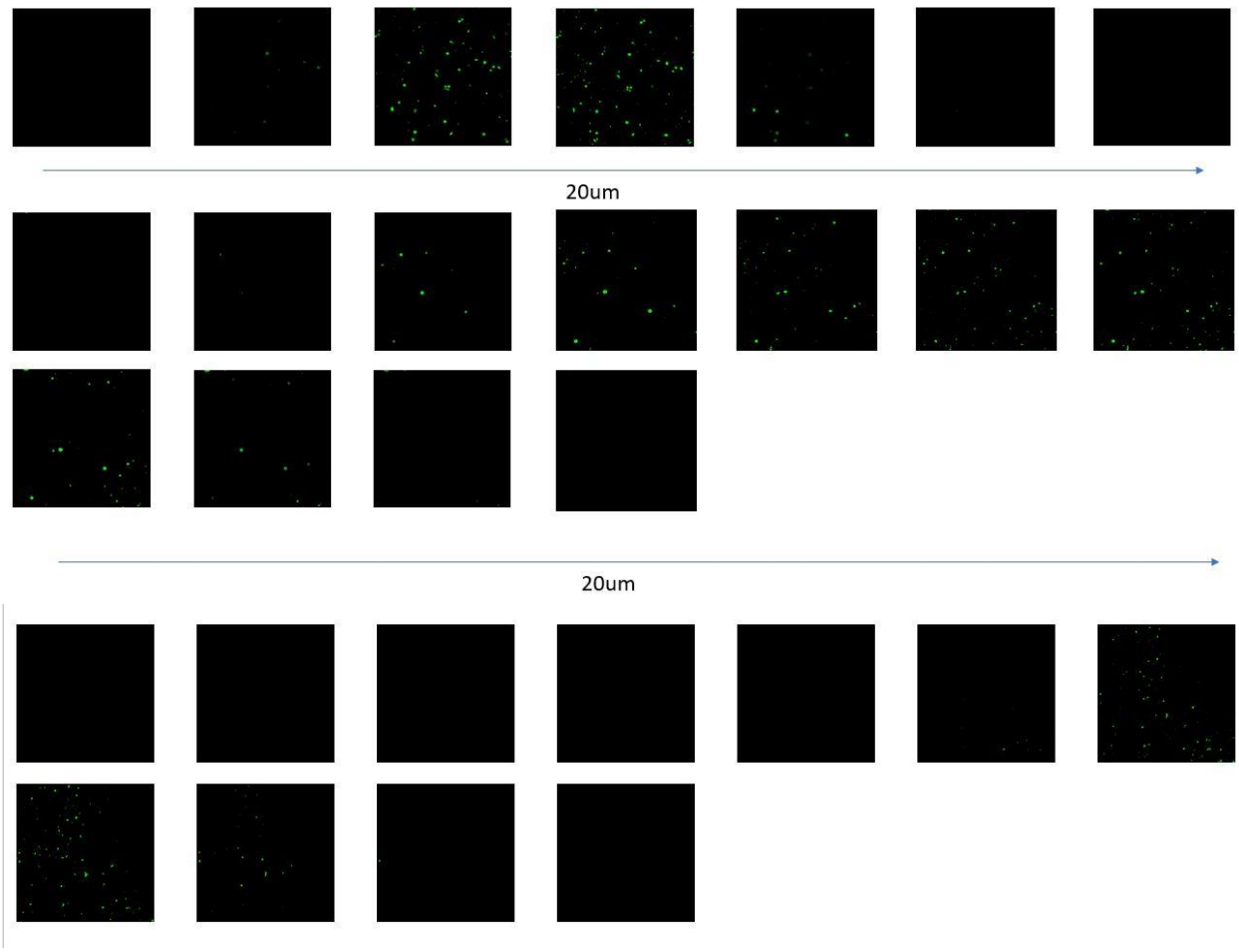

Figure 2.13 Typical Z-stack Fluorenes image for migration with OPN and CXCL12

The distance between each figure is 20 um. The first, second and third lines represent HUVECs culture 2/7/10 days on scaffold with il1-bate treatment. The statistic results are down below.

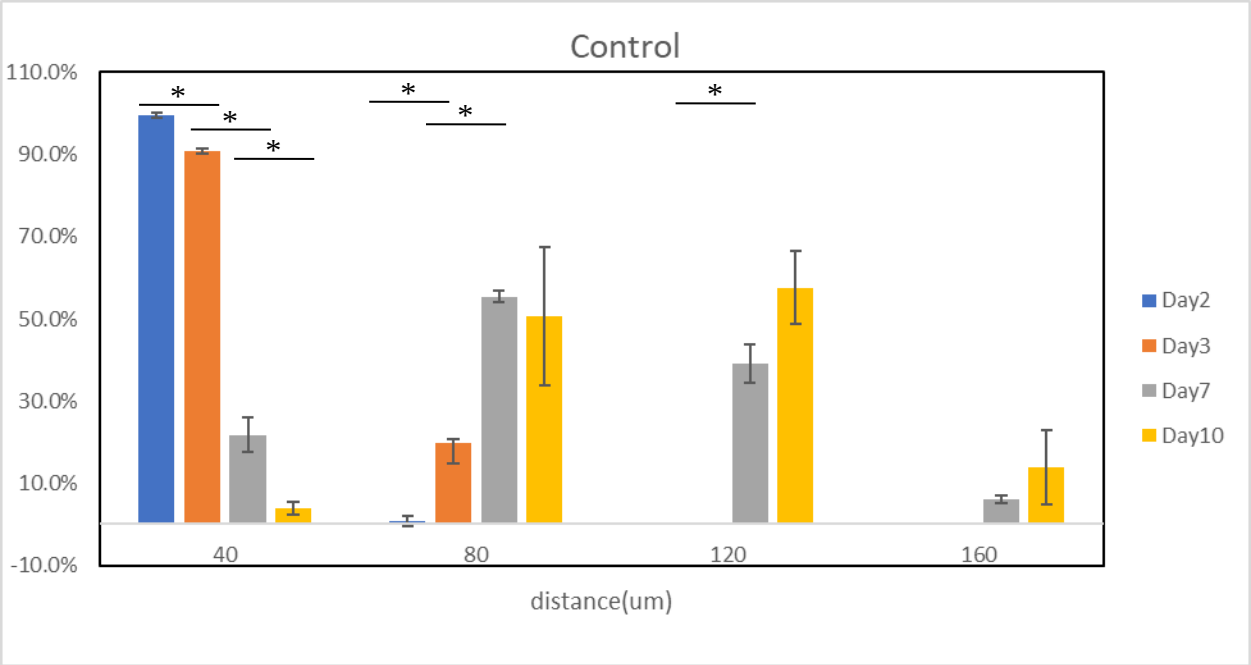
Control
110.0%
90.0%
70.0%
50.0%
30.0%
10.0%
-10.0%
40
80
120
160
distance(um)
Day2
Day3
Day7
Day10

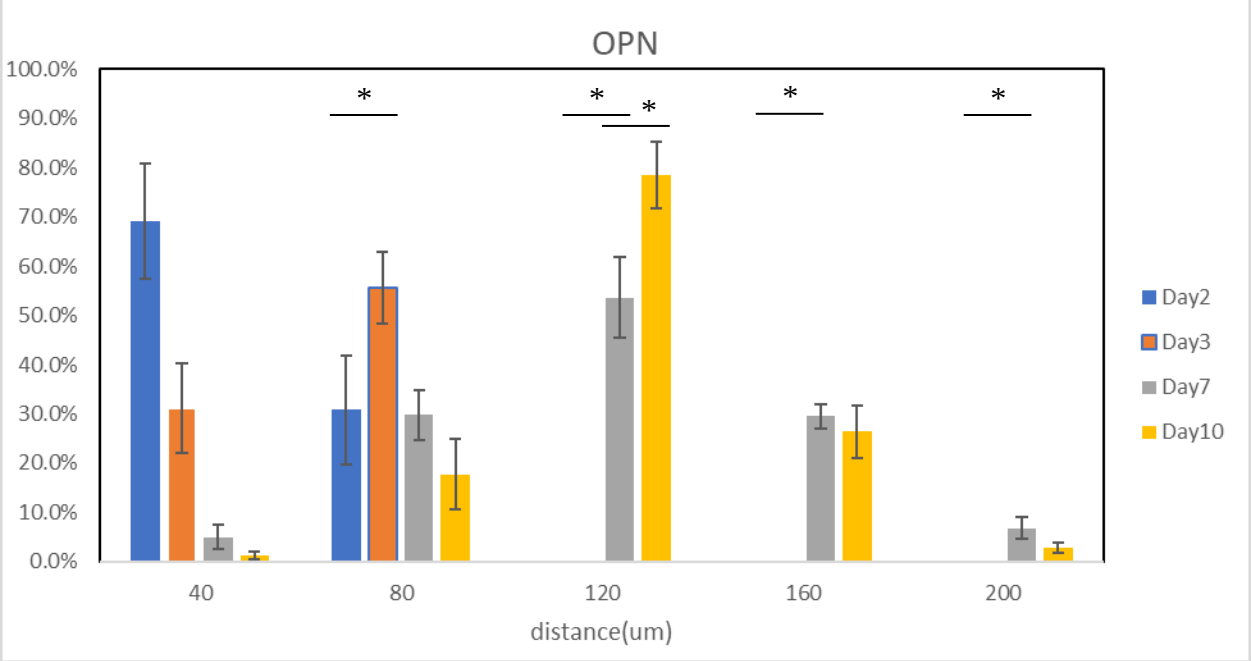
OPN
100.0%
90.0%
80.0%
70.0%
60.0%
50.0%
40.0%
30.0%
20.0%
10.0%
0.0%
40
80
120
160
200
distance(um)
Day2
Day3
Day7
Day10

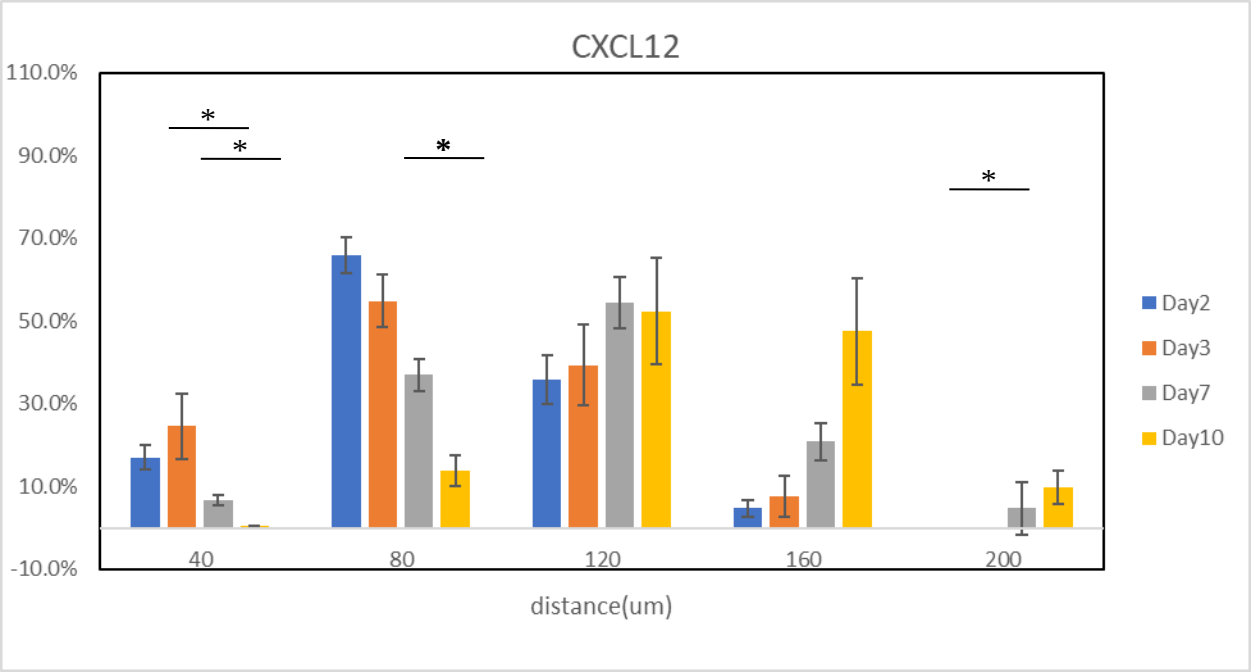

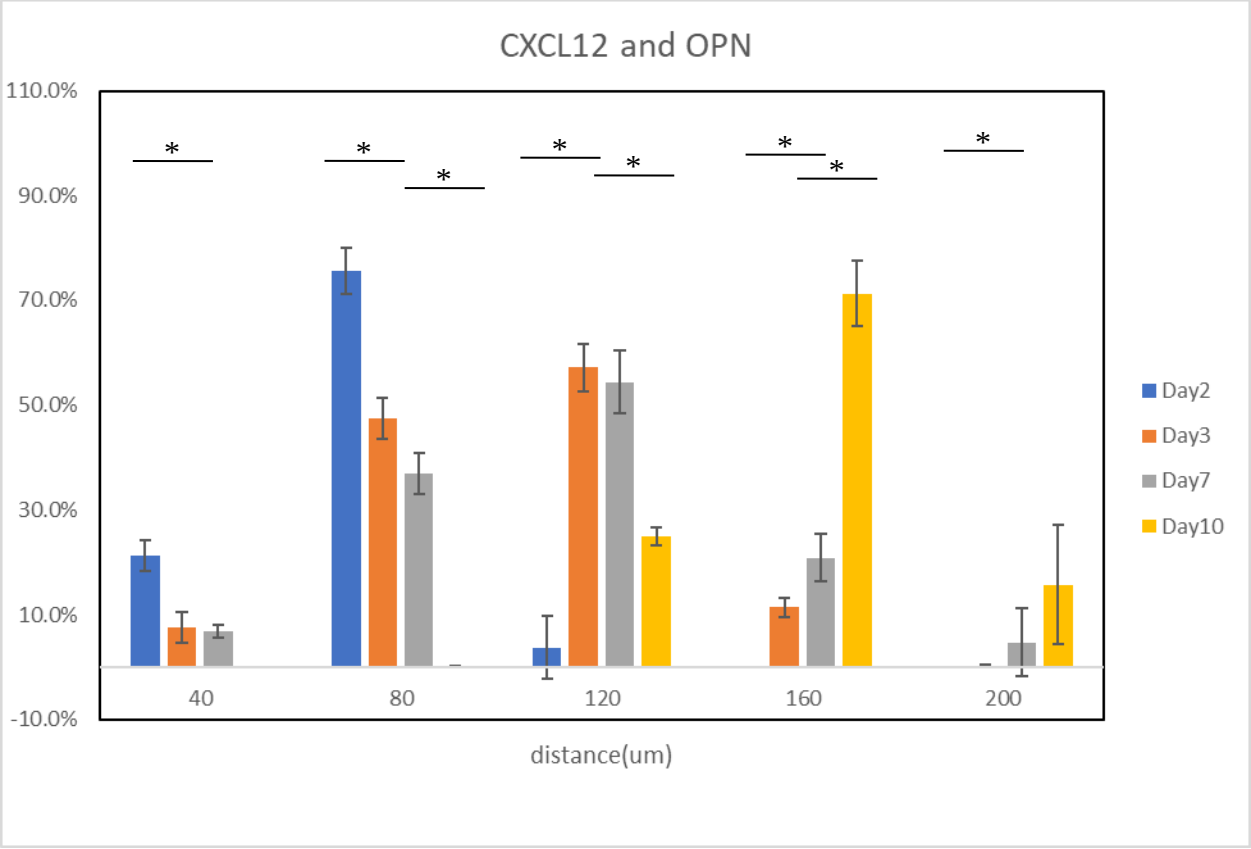

Figure 2.14 HUVECs migration distance

With the treatment of OPN and CXCL12, the HUVECs migration distance increased in PCL scaffold. With only one growth factors treatment also could affect the migration distance but not as much effective as both. Cause the migration data similar with bell curve, Figure 2.15b shown the average migration of each sample at each time points to do comparison.

2.9 In Vivo Results

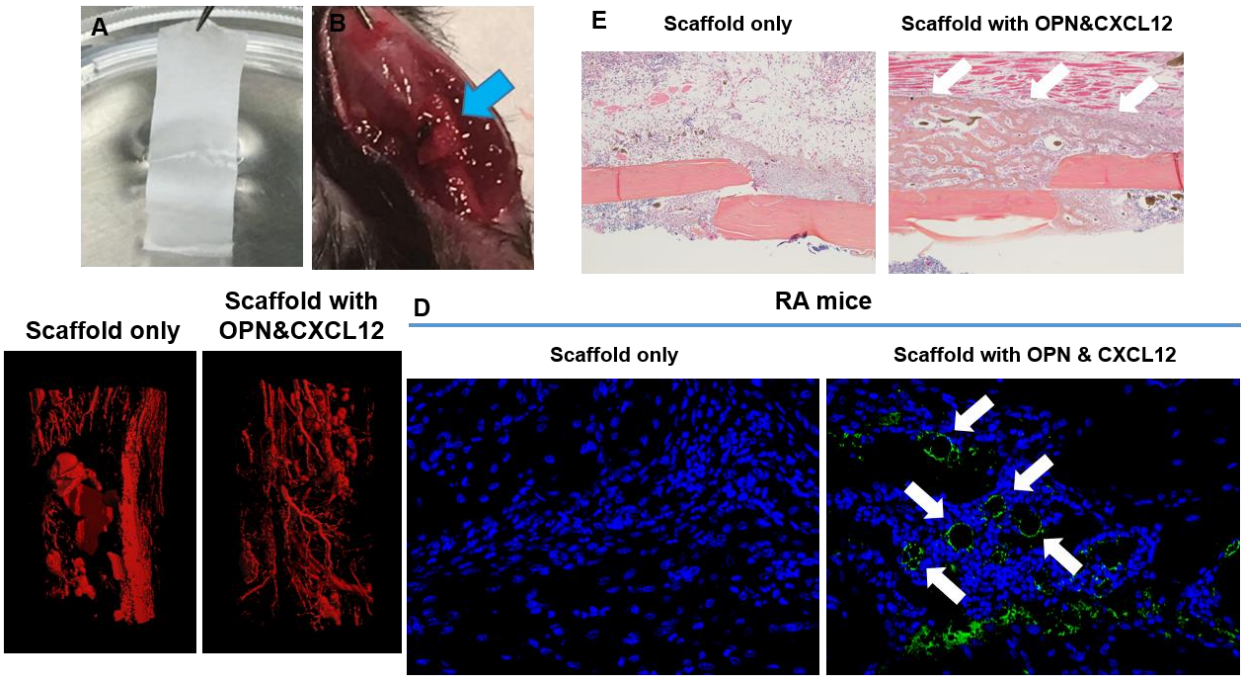

Figure 2.16 Supply with OPN and CXCL12 restores angiogenesis and facture union in RA mice

According to figure 2.16, figure A and B is PCL scaffold with OPN and CXCL12 microsphere and without any protein applied to bone fracture in Rheumatoid Arthritis mice with 5 repeats. The figure C is results of angiogenic microCT of D10 RA callus, which shows with the treatment

of OPN and CXCL12, angiogenesis restoration occurred. This result matched the hypothesis for OPN&CXCL12 microspheres-Scaffold system. In figure D, endomucin immunofluorescent staining shows type H vessel is increased by treatment of OPN and CXCL12. Figure E is results of histological analyses of D10 fracture callus. The bony callus bridging can be observed in OPN and CXCL12 treatment group. Based on the results in vivo, we can proved that OPN and CXCL12 microsphere indeed improved repaired of bone fracture in RA mice.

Chapter 3 Fabricated PCL Scaffold with ADSCs

3.1 Method

3.1.1 Culture ADSCs cells

ADSCs were cultured in MEMa with 10% FBS and 1% Penciling. The cells were separated from flask by adding trypsin and dilute into 3M/ml in medium with 2% gelatin to make precursor for electro-spinning.

3.1.2 Fabricated process

Firstly, sterile electro-spinning chamber and all equipment for preventing from contamination. The ADSCs and gelatin solution was injected into the metal electro-spinning needle through sterile syringe A by pump A vertical with collector and keep the inject rate in 10ml/h. Inject 10% PCL solution into the metal electro-spinning needle through syringe B by pump B horizontal with the collector.

3.1.3 Characterized Process

The PCL scaffold with ADSCs samples collected during the culture from 1 to 7 days by slide glass mounting with CC mount and covered with glass for short term storage. For the cross section, the PCL scaffolds were immersed in liquid nitrogen and cut before unfrozen. Image of the microspheres were obtained with a Zeiss 510 META laser scanning confocal microscope.

The laser absorbance wavelength for Green fluorescent protein in ADCSs is 395nm. The resolution for florescence capture image is 1920*1920 pixels with Z-stack mode. The figure did post processed and edited by image J software.

The structure of scaffold with microsphere were shown by SEM image. After the process of vacuum-dried, with sputter gold coated to increase conductivity, cutting in liquid nitrogen then observed under SEM at an acceleration voltage of 5kV to characterize the morphology of the scaffolds with ADSCs.

3.1.4 Cells Proliferation

The scaffold with ADSCs were cultured in MEMa with 10% FBS and 1% Penciling in flasks. The sample of same volume and weight were collected in 1 to 7 days for confocal image and tested the DsDNA content in the scaffolds with 3 repeats.

3.2 Characteristic image

3.2.1 SEM image

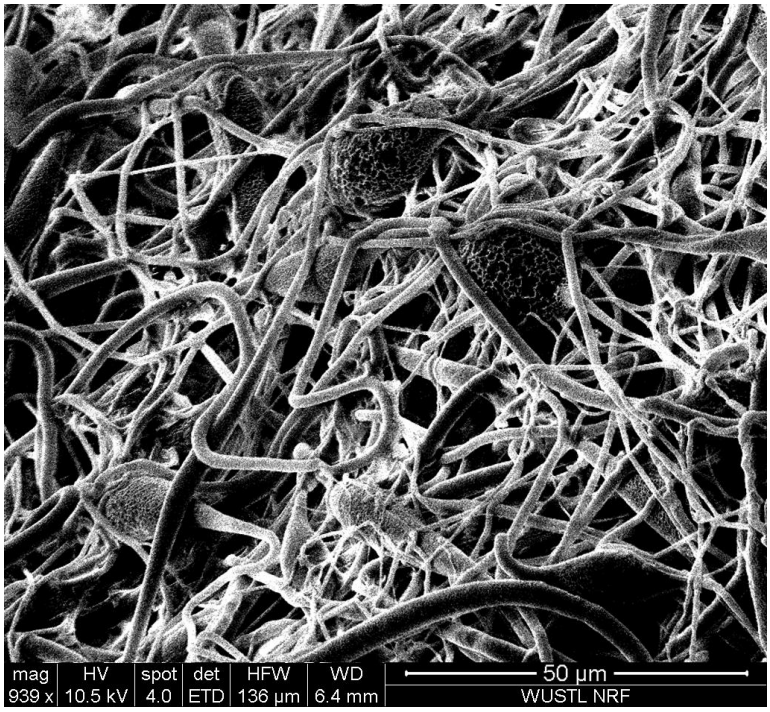

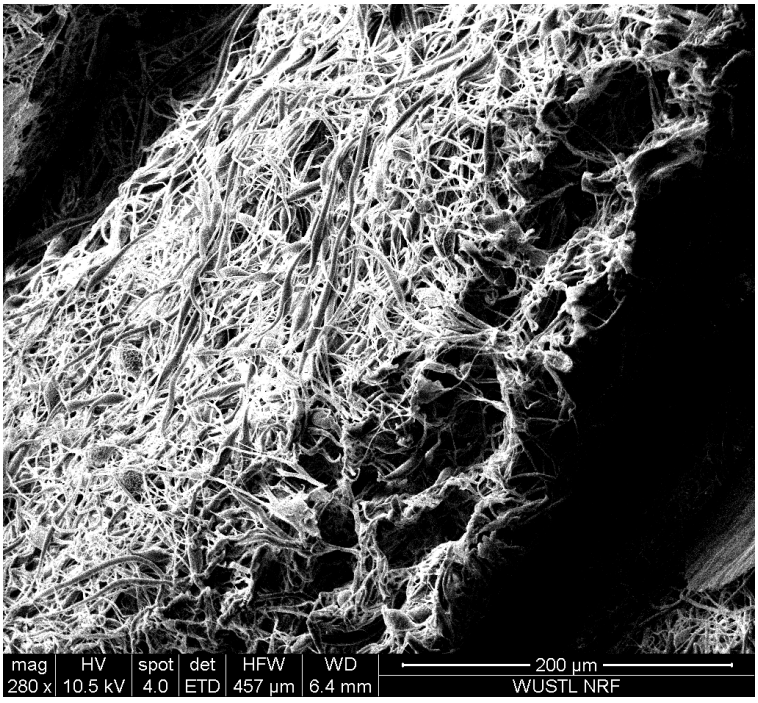

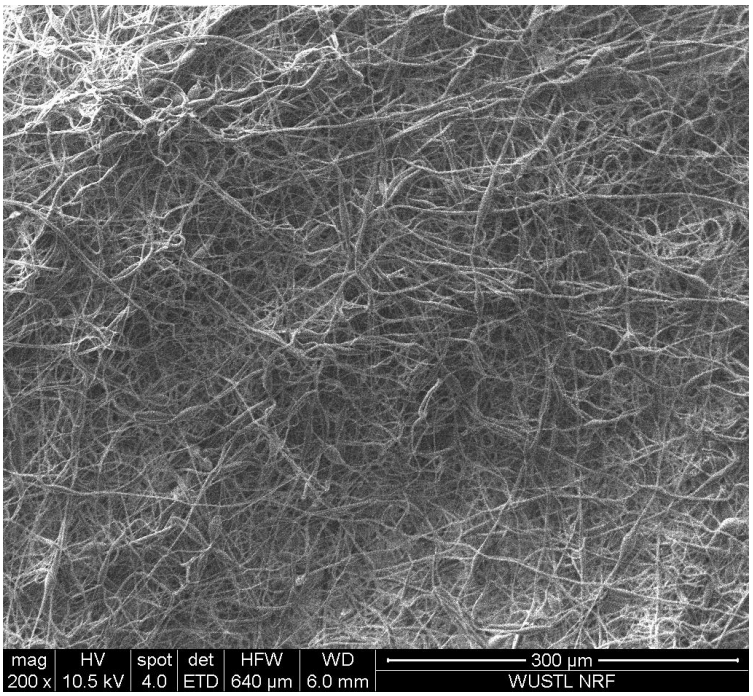

Figure 3.1 SEM image for cross section and surface

Figure B is the SEM image of cross section of PCL scaffolds with ADSCs after frozen-dry, figure C is the surface of PCL scaffold with ADSCs after frozen-dry. The fiber is uniform and barely any bead formation in scaffold. Based on figure A, we can observe ADSCs was wrapped in fibers. The surface of cells is wrinkled compare with beads on fibers, which can prove that spheres are not beads on fibers but ADCSs in scaffold. The density of cells is lower than expectation might since ADSCs might drop off from hydrophilic PCL scaffold cause by process of frozen-dry.

3.2.2 Confocal microscopy image

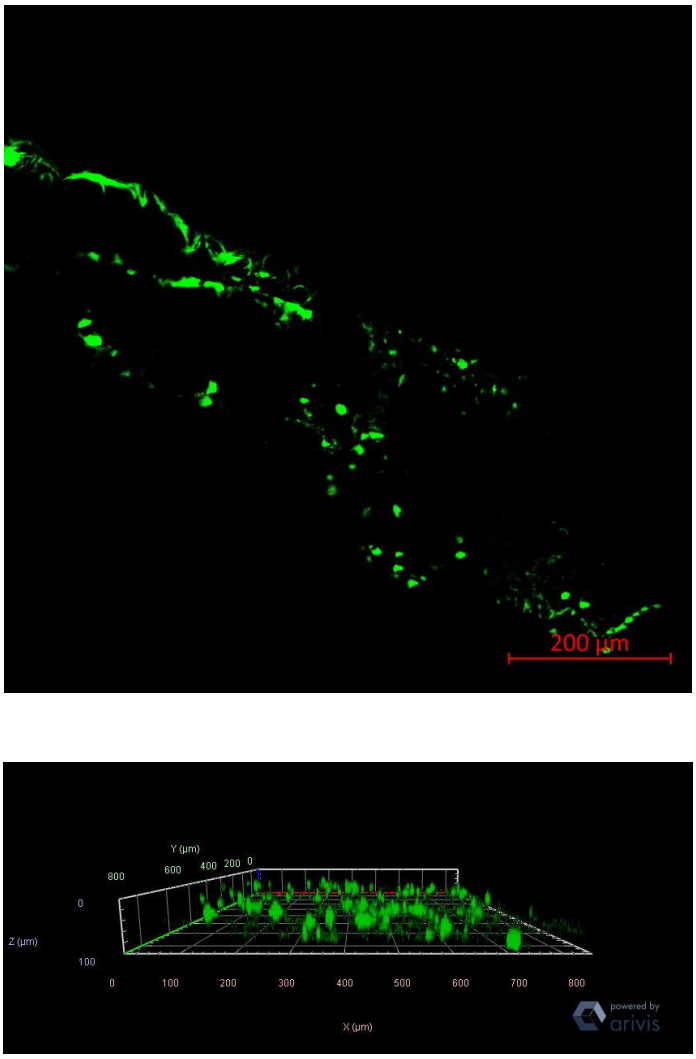

Figure 3.2 Confocal image for cross section and surface

The figure 3.2 shown the confocal microscopy image of ADSCs in PCL 3D scaffold after fabricated and cultured after 1 day. The figure 3.2A is the image of cross section cutting image by frozen the scaffold in liquid nitrogen and cut directly. The figure 3.2B is the horizontal cross section image by scanning Z stack florescence single and combined into 3D image. The width of scaffold with ADSCs was round 200 um based on SEM image and florescence image. Based on the image of confocal and SEM, this result demonstrated that the electro-spinning method is efficient in the fast fabrication of tissue regenerated scaffold with cells.

3.3 Cells growth in PCL scaffold

3.3.1 Confocal Image

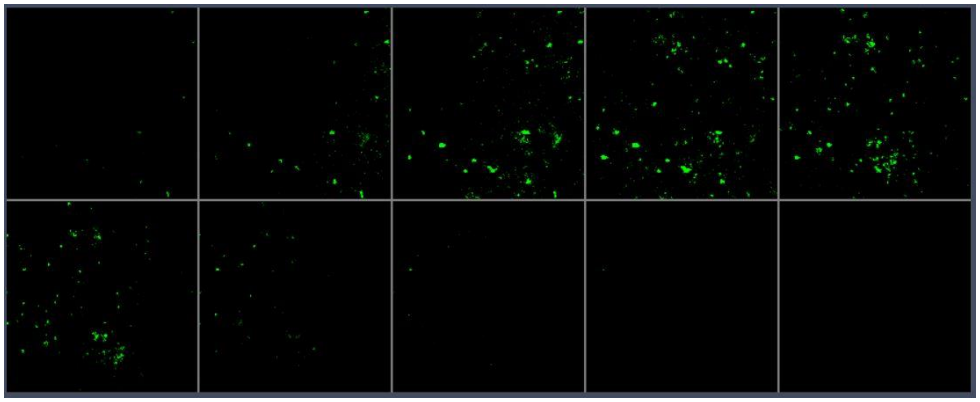

[Figure 3.3A Z-stack image of scaffold after 1 day of culture]

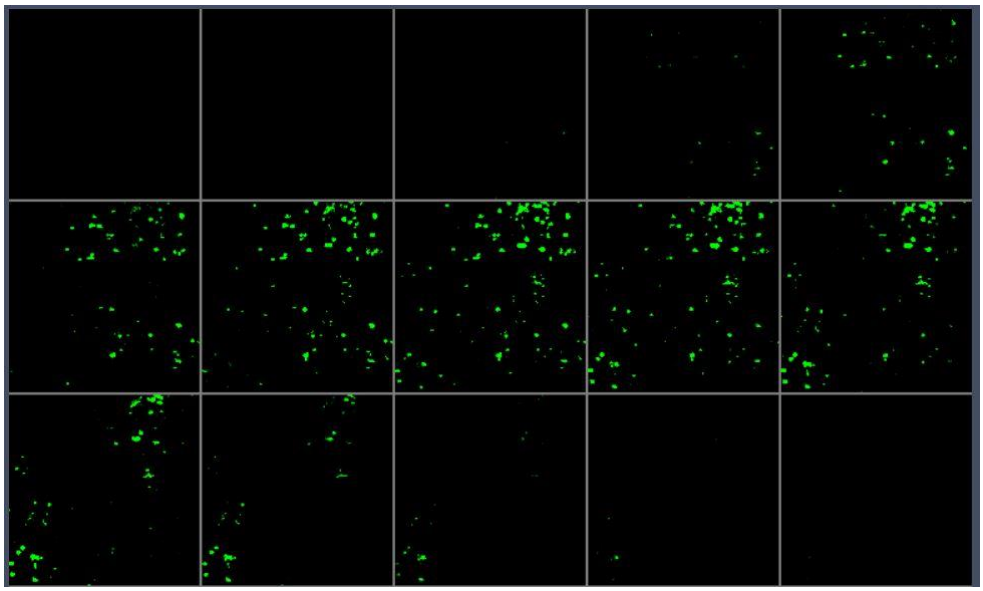

Figure 3.3B Z-stack image of scaffold after 4 days of culture

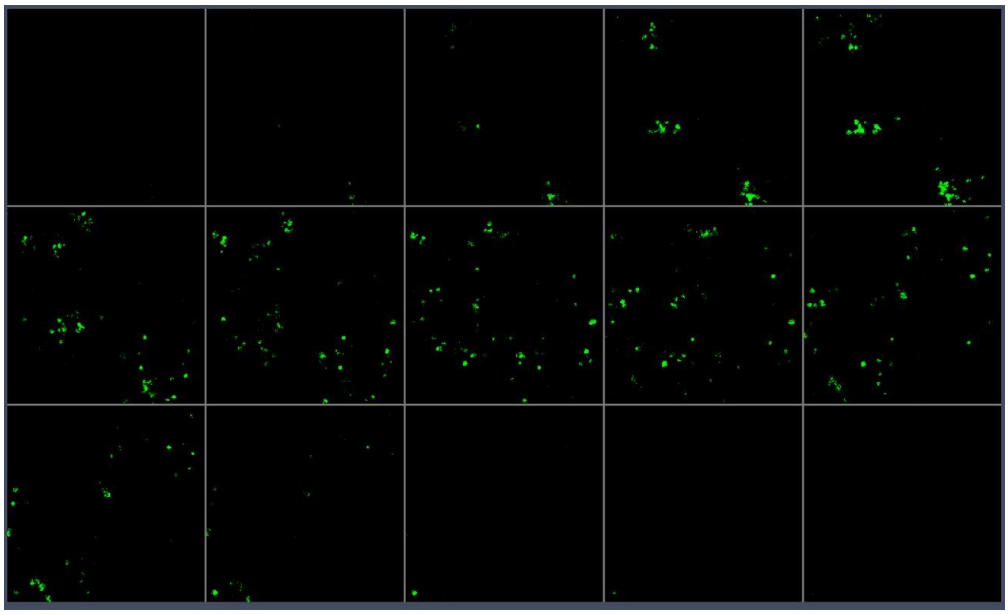

Figure 3.3C Z-stack image of scaffold after 7 days of culture

Figure 3.3 represent typical confocal fluorenes microscope images of ADSCs with GFP single in each layer in PCL scaffold. All group of images started from the surface of the scaffold, the distance between each image are 10 um. We can observe that ADSCs still exists after cultured of 7 days. The quantification data will be shown below.

3.3.2 DsDNA Results

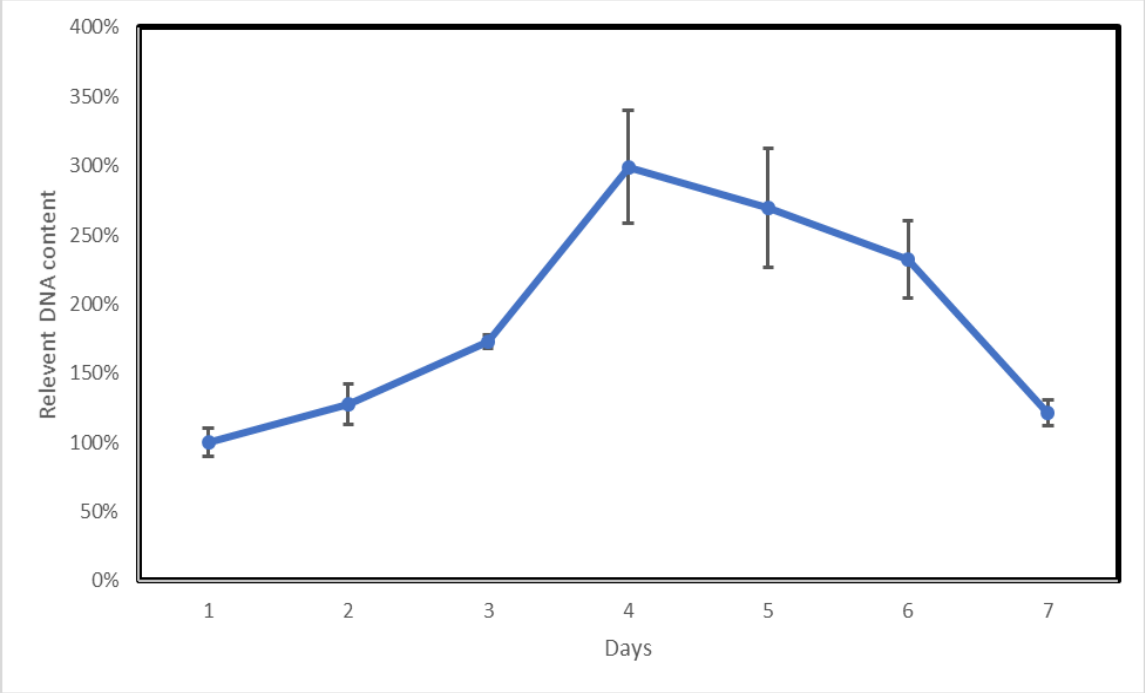

Figure 3.4 Relative DsDNA content of scaffold with ADSCs

The mainly concern of electro-spinning is the surival of stem cells under high voltage. This movtiavted us to explore the cells prolification after scaffold fabrictaed. Figure 3.4 shown the DsDNA content in scaffold culture in flasks. The ADSCs increased their DsDNA content for live cells during the culture at first 4 days, and decrease DsDNA content from 4 to 7 days. At day 4, the DsDNA reached pick amount. The reason may caused by nutrition in culture medium can not reach the middle of the scaffold. Also, the medium for electro-spray had gelatin, which may have the ability to protect ADSCs under high voltage and in organic solvent.

Conclusion

The PCL fibrous scaffold fabricated via electro-spinning reached the stiffness for bone fracture repaired. We created PCL scaffold with CXCL12 and OPN encapsulated microspheres. In vitro and in vivo studies demonstrated that this scaffold could improve cells migration and proliferation, and eventually fast angiogenesis.

The PCL scaffold with ADSCs can be fabricated under high voltage and could survive over 7 days based on characterization results and DsDNA results. These 3D scaffold may have potential to engineer tissues for various applications.

References/Bibliography/Works Cited

[1] Nillesen, S. T. M.; Geutjes, P. J.; Wismans, R.; Schalkwijk, J.; Daamen, W. F.; van Kuppevelt, T. H. Biomaterials 2007, 28, 1123−1131.

[2] Singh, S.; Wu, B. M.; Dunn, J. C. Y. Biomaterials 2011, 32, 2059−2069.D. Tissue Eng. 2006, 12, 2093−2104.

[3]Laschke, M. W.; Harder, Y.; Amon, M.; Martin, I.; Farhadi, J.; Ring, A.; Torio-Padron, N.; Schramm, R.; Rücker, M.; Junker, D.; Häufel, J. M.; Carvalho, C.; Heberer, M.; Germann, G.; Vollmar, B.; Menger, M. D. Tissue Eng. 2006, 12, 2093−2104.

[4]Cleland, J. L.; Duenas, E. T.; Park, A.; Daugherty, A.; Kahn, J.; Kowalski, J.; Cuthbertson, A. J. Controlled Release 2001, 72, 13−24.

[5] Zisch, A.; Schenk, U.; Schense, J.; Sakiyama-Elbert, S.; Hubbell, J. J. Controlled Release 2001, 72, 101−113.

[6] Guo, Xiaolei, Elliott, Christopher G., Li, Zhenqing, Xu, Yanyi, Hamilton, Douglas W., Guan, Jianjun. Biomacromolecules 2012/10/08, 1525-7797

[8] Whalen, G. F.; Shing, Y.; Folkman, J. Growth Factors 1989, 1, 157−164.

[9] Fujita, M.; Ishihara, M.; Simizu, M.; Obara, K.; Ishizuka, T.; Saito, Y.; Yura, H.; Morimoto, Y.; Takase, B.; Matsui, T.; Kikuchi, M.; Maehara, T. Biomaterials 2004, 25, 699−706.

[10] Ekaputra, A. K.; Prestwich, G. D.; Cool, S. M.; Hutmacher, D. W. Biomaterials 2011, 32, 8108−8117.

[11] Chu, H.; Gao, J.; Chen, C.-W.; Huard, J.; Wang, Y. Proc. Natl. Acad. Sci. U.S.A. 2011, 108, 13444−13449.

[12] Zhang, M, Kiratiwongwan, T, Shen, W. J Biomed Mater Res. 2019; 1– 10.

[13] Begoña Almería, Weiwei Deng, Tarek M. Fahmy, Alessandro Gomez, Journal of Colloid and Interface Science, Volume 343, Issue 1, 2010, Pages 125-133

[14] Maeda, Y., Yonemochi, Y., Nakajyo, Y. et al. Sci Rep 7, 3305 (2017)

[15] Wang, C., Abu-Amer, Y., O'Keefe, R.J. and Shen, J. (2018), J Bone Miner Res, 33: 283-297

[16] Jianjun Guan, Feng Wang, Zhenqing Li, Joseph Chen, Xiaolei Guo, Jun Liao, Nicanor I. Moldovan, Biomaterials, Volume 32, Issue 24, 2011, Pages 5568-5580

[17] R.A. Jain, Biomaterials 21 (2000) 2475.

[18] M.L. Hans, A.M. Lowman, Curr. Opin. Solid State Mater. Sci. 6 (2002) 319.

[19] R.M. Mainardes, L.P. Silva, Curr. Drug Targets 5 (2004) 449.

[20] T.M. Fahmy, P.M. Fong, A. Goyal, W.M. Saltzman, Mater. Today 8 (2005) 18.

[21] S.M. Moghimi, A.C. Hunter, J.C. Murray, Pharmacol. Rev. 53 (2) (2001) 283.

[22] O.C. Farokhzad et al., PNAS 103 (16) (2006) 6315.

[23] R. Sinha et al., Mol. Cancer Ther. 5 (8) (2006) 1909.

[24] H. Takeuchi, H. Yamamoto, Y. Kawashima, Adv. Drug Delivery Rev. 47 (1) (2001) 39.

[25] S.H. Kim, Langmuir 21 (19) (2005) 8852.

[26] Jiajia Xue, Min He, Hao Liu, Yuzhao Niu, Aileen Crawford, Phil D. Coates, Dafu Chen, Rui Shi, Liqun Zhang, Biomaterials, Volume 35, Issue 34, 2014, Pages 9395-9405,

[27] Bei Feng, Shoubao Wang, Dongjian Hu, Wei Fu, Jinglei Wu, Haifa Hong, Ibrahim J. Domian, Fen Li, Jinfen Liu, Acta Biomaterialia, Volume 83, 2019, Pages 211-220

[28] Maria Doitsidou, Michal Reichman-Fried, Juürg Stebler, Marion Köprunner, Julia Dörries, Dirk Meyer, Camila V. Esguerra, TinChung Leung, Erez Raz, Cell, Volume 111, Issue 5, 2002, Pages 647-659, ISSN 0092-8674,

[29] Katarina Wolf, Stephanie Alexander, Vivien Schacht, Lisa M. Coussens, Ulrich H. von Andrian, Jacco van Rheenen, Elena Deryugina, Peter Friedl, Seminars in Cell & Developmental Biology, Volume 20, Issue 8, 2009, Pages 931-941, ISSN 1084-9521